STRESS RELIEF IN CALCIA PARTIALLY-STABILISED ZIRCONIA

THERMAL SHOCK INDUCED MICROSTRUCTURAL MODIFICATIONS AND MECHANISMS OF STRESS RELIEF IN CALCIA PARTIALLY-STABILISED ZIRCONIA

by

Ahmed M. El-Shiekh, B.Sc.

A Thesis
Submitted to the School of Graduate Studies
in Partial Fulfilment of the Requirements
for the Degree
Master of Engineering

McMaster University
October, 1972

MASTER OF ENGINEERING
(Metallurgy and Materials Science)

McMASTER UNIVERSITY
Hamilton, Ontario

TITLE: Thermal Shock Induced Microstructural Modifications and Mechanisms of Stress Relief in Calcia Partially-Stabilised Zirconia.

AUTHOR: Ahmed M. El-Shiekh, B.Sc., Cairo University

SUPERVISOR: Dr. P. S. Nicholson

NUMBER OF PAGES: ix, 104

ABSTRACT

The stress relieving mechanisms in two different batches of thermal-shock resistant calcia-PSZ have been investigated. The nature of the stress relief in the two materials appears to result from the transformation of the pure ZrO_2 component of the microstructure at temperatures below, within, and above the normal transformation temperature range. In the batch #1 material, which contains a larger volume fraction of monoclinic phase, the cubic matrix material behaves in a "brittle" fashion resulting in the production of a high density of microcracks in the body. The density of these cracks is such that the level of energy that can be stored in the body is limited and thermal shock resistance results. The batch #2 material contains considerably less monoclinic material and the evidence suggests that the cubic matrix within it can act in a ductile fashion. This ductility together with the twinning of the monoclinic component of the microstructure possibly relieves the stresses developed in the material on thermal shock.

In the batch #2 material, large platelets were observed to develop following thermal cycling from temperatures above those of the normal transformation. It has been demonstrated that stress plays a major role in the development of these features. In view of the possible ductility of the cubic matrix in this material it is suggested that the thermal cycling "works" the material, texturing the pure zirconia component in it, so leading to the development of the observed platelets.

ACKNOWLEDGMENTS

The author wishes to express his gratitude to his supervisor, Dr. P. S. Nicholson, for his encouragement and continuous guidance throughout the course of this work.

The author also wishes to thank Dr. J. D. Embury, Dr. R. Kelly and Mr. C. Sargent (Visiting Professor) for their valuable suggestions and constructive criticism; Dr. A. Heuer (Case Western Reserve University) for his electron micrographs; and Miss L. de Jong for typing the thesis.

The financial assistance of McMaster University, in the form of a teaching assistantship, and of the Atomic Energy of Canada Limited, in the form of a research grant to Dr. Nicholson, are also gratefully acknowledged.

TABLE OF CONTENTS

LIST OF FIGURES

CHAPTER I

INTRODUCTION

Because of the importance of ZrO_2 in severe environments, considerable attention has been given to the properties of this material. Pure zirconia is known to exist in three crystalline modifications, namely: monoclinic (up to about 1100°C), tetragonal (1100° - 2100°C) and cubic (2100°C to melting point).

The practical usage of pure zirconia is severely restricted by its polymorphism, for thermal cycling through the transition temperature causes cracking and sometimes complete disintegration of the specimen.

Zirconia can be "stabilized" in the high temperature cubic form by forming solid solutions with CaO, MgO or Y_2O_3. This eliminates the disruptive phase transformation. However, the thermal expansion coefficients of such stabilized zirconias, which are $\sim 12 \times 10^{-6}/^{\circ}C$, are high(1) and, together with the very low thermal conductivity of zirconia(2), this results in very poor thermal shock behaviour. On the other hand, partially stabilized zirconia (PSZ) has superior thermal shock resistance compared with the fully stabilized material.

The exceptional thermal shock resistance of PSZ indicates the existence of stress relieving mechanisms in this material, which reduce the damage associated with severe thermal shock. Possible sources of stress relief are:

(a) Occurrence of the monoclinic-tetragonal zirconia transformation (at sub-transition temperatures) during thermal shocking.

(b) The onset of twinning which has been observed to operate in normal zirconia.

(c) The microcracking mechanism as suggested by Karaulov et al(3). They considered that microcracking caused by the phase inversion of zirconia, when the material was cycled through the transition region, was responsible for the high thermal shock resistance of this material. They observed annular microcracks, 20 - 40 microns wide around the grains. These workers, however, used impure zirconia (97%). The major impurities were Al_2O_3 and SiO_2. Garvie and Nicholson(4) speculated on the nature of this mechanism, suggesting that such material would have appreciable quantities of calcia-alumino-silicates in the grain boundaries which could give rise to the annular microcracking observed by Karaulov et al.

(d) The intrinsic stress-relief mechanism. King and Javorsky(5) suggested that PSZ has an important capacity for stress relief through the mechanism of plastic deformation. They offered optical photomicrographic evidence that an intrinsic stress relieving mechanism existed in this material. They observed formation of slip bands around pores and pure zirconia grains. They did not investigate the mechanism of production of these slip bands. Garvie(6) suggested that these slip bands are due to the presence of pure zirconia in the system. According to Garvie, thermal stresses could cause transformation of the monoclinic to tetragonal phase to occur at sub-transition temperatures under thermal shock conditions.

Hart and Chaklader(7) observed superplasticity in pure zirconia during the inversion. They suggested that the superplasticity of the monoclinic domains in the monoclinic-cubic hybrid phase is responsible for the stress relief observed by King and Javorsky. The cubic phase alone cannot possess stress-relieving mechanisms because it becomes quite brittle as the monoclinic phase disappears with increasing stabilizer content(5).

This work will deal mainly with the investigation of which mechanism or combination of mechanisms is responsible for the stress relief in this material. Lime-partially stabilized zirconia was chosen in view of the instability of the magnesia-stabilized material(8).

CHAPTER II

LITERATURE REVIEW

2.1 Zirconia

There are three well-defined polymorphs of pure zirconia, namely the monoclinic, tetragonal and cubic structures. The monoclinic phase is stable up to about 1100°C and then transforms over about a 100°C temperature range to the tetragonal phase. Both these structures are related to the fluorite structure. Finally, at about 2370°C, the compound adopts the cubic fluorite structure. The fact that ZrO_2 crystallizes in the fluorite structure is inexplicable in terms of modern crystal chemistry. For example, Wells(9) asserts that the rutile structure is the stable form of binary ionic compounds of the type RX_2 when the radius ratio is in the range 0.414 - 0.732; and the radius ratio of ZrO_2 is 0.57, well within the rutile field. Evidently, the stable structure is governed by considerations other than the simple radius ratio and Bendoraitis and Salomon(10) have suggested that there is appreciable covalent bonding in ZrO_2 which might explain the discrepancy.

2.1.1 Monoclinic ZrO_2

The crystal structure of monoclinic zirconia has been of interest since the early work of Yardley (Lonsdale)(11) in 1926. She determined the space group to be $P2_1/C$ and showed that the unit cell contained 4 ZrO_2. The suggestion was made that the structure was probably a distorted fluorite, but a definite structure was not proposed. Using Yardley's data, Na'ray Szabo (1936)(12) proposed a structure which, however, had unsatisfactory packing and unreasonable bond distances. McCullough and Trueblood (1959)(13) collected new data from some natural crystal fragments which appeared free of the twinning that is present in most, if not all, natural crystals. They obtained the following crystallographic data:

a	5.169 Å
b	5.232 Å
c	5.341 Å
β	99° 15'
Unit cell volume	142.36 $\AA^3$
Density	5.826 gm/cc

The zirconium ions are in seven-fold co-ordination, sandwiched on one side by oxygen ions in tetrahedral co-ordination (O_{II}) and on the other side by oxygen ions in triangular co-ordination (O_I). A somewhat idealized picture of the co-ordination polyhedron is given in Figure 1. Smith and Newkirk (1965)(14) refined the crystal structure using X-ray data collected from a synthetic single crystal.

The high temperature elastic constants for fully dense polycrystalline monoclinic ZrO_2 were calculated by Smith and Crandall(15) from sonic data. The data were fitted by an equation of the following

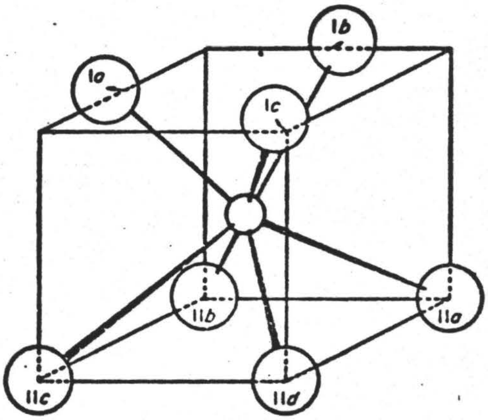

FIGURE 1.The Zr coordination polyhedra in baddeleyite (idealized) [McCullough and Trueblood, 1959].

form:

$$E = E_o \exp(-b_1 P)$$

where: E_o = Young's or shear modulus at zero porosity
E = Young's or shear modulus at some porosity, P
b_1 = an empirical constant
P = fractional porosity.

Typical data are given in Table 1.

The axial thermal expansion of zirconia was first measured by Campbell and Grain(16). Their data are summarized in Table 2. Lang et al(17) measured the axial thermal expansion of monoclinic ZrO_2 and obtained good agreement with these data.

2.1.2 Tetragonal ZrO_2

The monoclinic structure is stable up to ≈ 1100°C on heating. After this it begins to transform to the tetragonal form. The transformation occurs over ≈ 100°C temperature interval; the transformation mechanism will be discussed in a later section.

The high temperature tetragonal form of ZrO_2 was first observed by Ruff and Ebert(18) during their studies on the polymorphism of ZrO_2 and its stabilization. Since that time it has been generally assumed that the tetragonal form represents a slightly distorted CaF_2 type structure. Teufer(19) determined the crystal structure of tetragonal zirconia and obtained the following data:

TABLE 1

Temperature, °C	E_o (psi × 10^{-6})	G_o (psi × 10^{-6})	b_1
25	35.43	13.96	3.544
1000	22.19	9.58	3.037

TABLE 2

Temperature, °C	a axis	b axis	c axis	β angle
264	$8.4 \times 10^{-6}\ {}^{\circ}\mathrm{C}^{-1}$	3.0	14.0	99° 11'
504	$7.5 \times 10^{-6}\ {}^{\circ}\mathrm{C}^{-1}$	2.0	13.0	99° 3'
1110	$8.7 \times 10^{-6}\ {}^{\circ}\mathrm{C}^{-1}$	1.9	13.6	98° 43'

$$a = b = 3.64\ \text{Å at } 1250^{\circ}\text{C}$$

$$c = 5.27\ \text{Å}$$

There are two molecules in the elementary cell. With the origin at $\bar{4}$ m2, the zirconium and oxygen atoms are located in positions similar to those found in the fluorite structure in:

2 Zr (a) 0, 0, 0; 1/2, 1/2, 1/2;

4 O (d) 0, 1/2, Z; 1/2, 0, $\bar{Z}$; 0, 1/2, 1/2 + Z; 1/2, 0, 1/2-Z.

where $Z_o = 0.185$. The parameter Z = 0.25 for the fluorite structure.

In tetragonal ZrO_2, each zirconium atom is surrounded by eight oxygen atoms, four at a distance of 2.065 Å in a flattened tetrahedron and four at 2.455 Å in an elongated tetrahedron which is rotated 90° relative to the former one. Each oxygen has two oxygen neighbors at 2.635 Å and four at 2.655 Å, and is bonded to two zirconiums at 2.065 Å, while two more Zr are 2.455 Å away. This combination of two distorted tetrahedra is similar to the zirconium silicate structure as measured by Krstanovic(20). Tetragonal ZrO_2 is isostructural with red HgI_2.

The axial thermal expansion of tetragonal zirconia was measured by Lang(21) between 1150° and 1700°C who obtained values:

$$a = 4.506 \times 10^{-5}\ \text{Å}/^{\circ}\text{C}$$

$$c = 7.576 \times 10^{-5}\ \text{Å}/^{\circ}\text{C}$$

2.1.3 Cubic Zirconia

Cubic zirconia has first been reported by Smith and Cline(22) by means of high temperature X-ray diffraction experiments. The structure was fluorite and the tetragonal-cubic reversible transformation was placed at 2285°C. The lattice parameter is 5.273 Å. The cubic phase could not be retained by quenching. Wolten(23) confirmed these results, also using high temperature X-ray diffraction.

2.2 MgO-ZrO_2 and CaO-ZrO_2 Systems

In this section, the MgO-ZrO_2 system will be briefly discussed. On the other hand, the CaO-ZrO_2 system will be considered in greater detail as the work here reported was concerned with this system. The purpose of including the MgO-ZrO_2 system in the discussion is to demonstrate its instability and so indicate why the CaO-ZrO_2 system was chosen for study.

2.2.1 The MgO-ZrO_2 System

The MgO-ZrO_2 system has received a lot of attention(8,24-27). All the reported results generally agree that the cubic field is v-shaped, terminating in the neighborhood of 1400°C. However, the data differ considerably concerning the precise location of the phase boundaries. Figure 2 shows the phase diagram obtained by Grain(27) to be considered the most reliable because he used well-crystallized pure oxide reagents

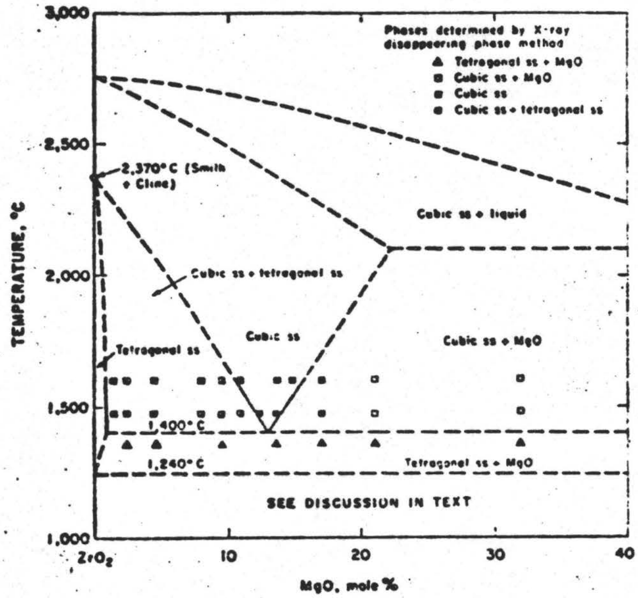

Fig. 2, Phase relations in a portion of the system ZrO_2-MgO (Grain, 1967)

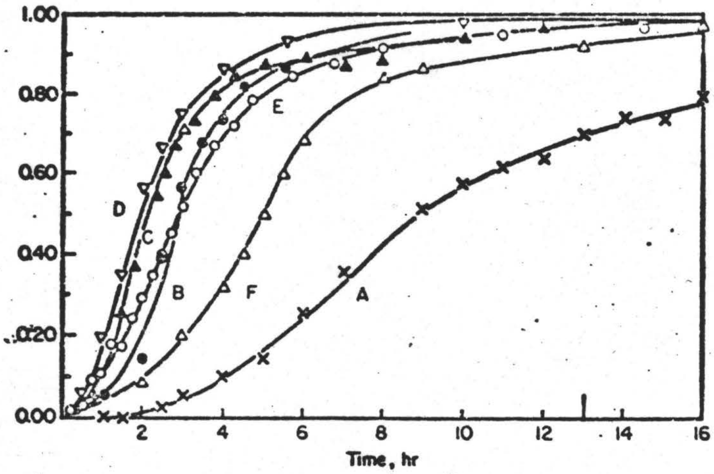

FIGURE 3, Effect of temperature on the decomposition of solid solutions of 80 mole % ZrO_2–20 mole % MgO. Solid solutions were prepared by heating for 1 hour at 1520°C and then were decomposed at (A) 1000°C, (B) 1075°C, (C) 1150°C, (D) 1250°C, (E) 1350°C, and (F) 1375°C (Viechnicki and Stubican, 1965).

and the sensitive X-ray lattice parameter technique to determine the boundaries.

The first investigation of the decomposition of cubic solid solution in this system was undertaken by Viechnicki and Stubican(8). They prepared 100% cubic solid solutions by rapidly quenching high temperature powders derived from co-precipitated gels. Samples of these powders were then isothermally decomposed between 1000° and 1400°C and the course of the decomposition monitored by X-ray diffractometry. Data showing the amount decomposed (α) as a function of time for various temperatures are given in Figure 3.

2.2.2 The $CaO-ZrO_2$ System

There have been many studies of the $CaO-ZrO_2$ system and the results can be divided into two groups. The first group considers that no $CaO-ZrO_2$ compound is formed in the cubic field. The range of existence of the cubic phase indicated by this group of workers is shown in Figure 4.

Duwez et al(24) reported the cubic field to lie between almost vertical straight lines, one at 16 and the other at 28 mole percent CaO. According to their work, the cubic phase extends from 2000°C down to room temperature. They utilised the disappearing phase method to determine these boundaries.

Dietzel and Tober(25) presented a much smaller cubic field composed of sloping boundary lines which intersected at about 1200°C. They also used the disappearing phase method.

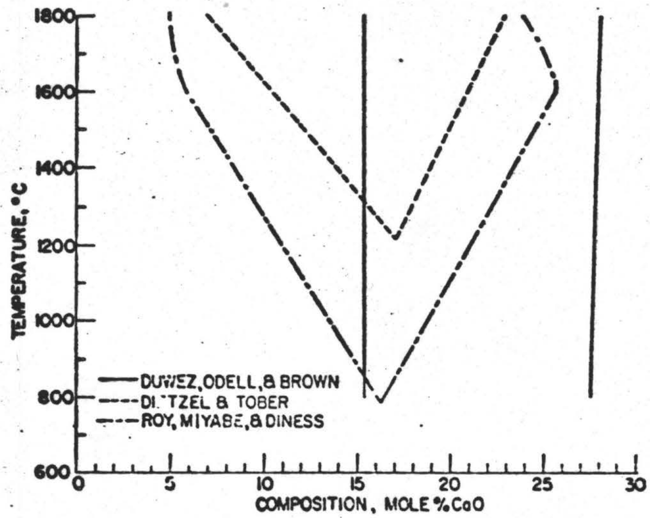

Fig.4. Cubic fields in the system CaO-ZrO$_2$ which show no compound formation.

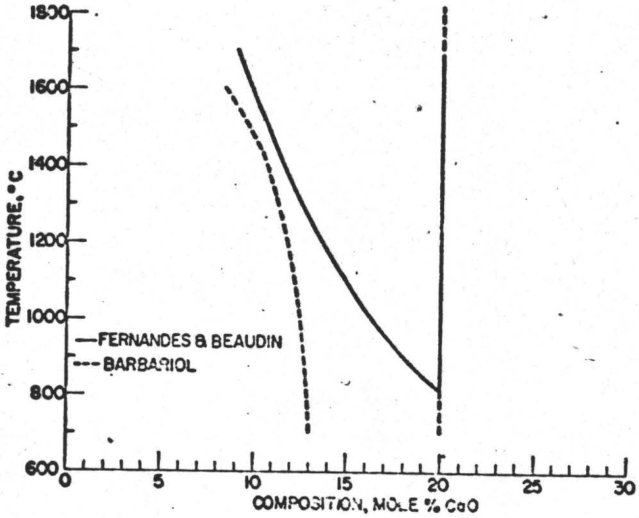

Fig.5. Cubic fields in the system Cao-ZrO$_2$ which show compound formation.

Roy et al(28) contributed the third version of the cubic field in this group. They obtained similar results as Dietzel and Tober, but the sloping boundary lines intersect at ≈ 800°C. They utilized the X-ray lattice parameter technique and mixed nitrates as reagents.

The second group of contributions considers a compound to form at the 20 mole percent CaO composition as shown in Figures 5 and 6.

Fernãndes and Beaudin(29) first postulated the existence of the compound $CaZr_4O_9$ at 20 mole percent CaO. They described the cubic field as consisting of a solution of ZrO_2 in $CaZr_4O_9$. These workers used both the disappearing-phase and lattice parameter methods. The reagents used were $CaCO_3$ and ZrO_2. Barbariol(30) also reported a vertical line at 20 mole percent CaO, indicating compound formation. He used the disappearing phase method and the same reagents as the previous workers.

Garvie(31) used the lattice parameter method and well-crystallized pure oxide reagents in his work on the extent of the cubic field. He reported that the cubic field may be described as originating from a solid solution series between cubic ZrO_2 and $CaZr_4O_9$. Further support for the co-existence of $CaZr_4O_9$ was discovered in the analogous CaO-HfO_2 system by Delamarre and Yorba(32) who discovered the compound $CaHf_4O_9$ in this system. The phase diagram suggested by Garvie is shown in Figure 6. This diagram is similar to that of Fernandes and Beaudin, although their cubic field extends to lower values of the temperature and composition than in the case of Garvie. This discrepancy is possibly due to the fact that Fernandes and Beaudin used $CaCO_3$ as a reagent.

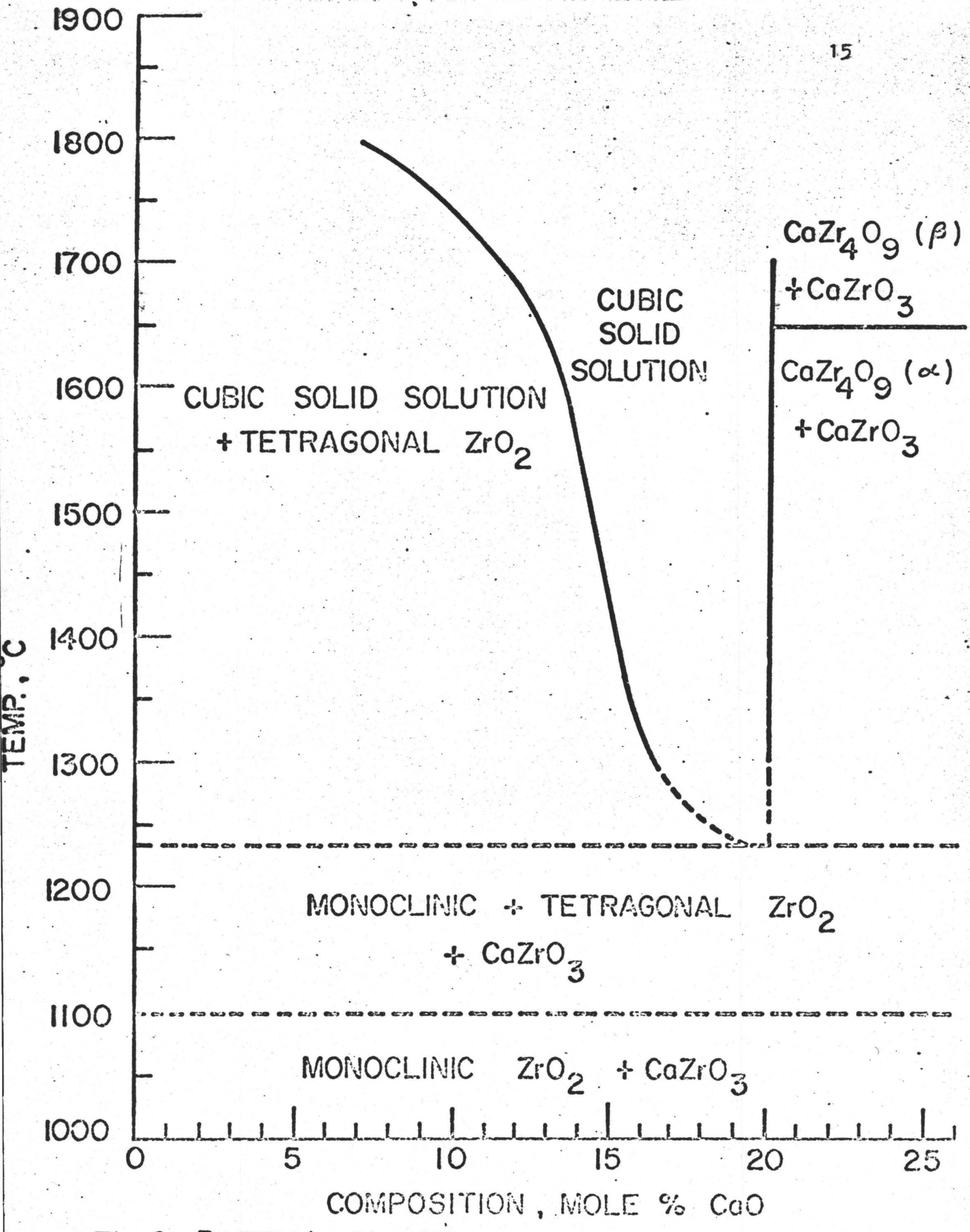

Fig. 6 PARTIAL PHASE DIAGRAM FOR THE CaO-ZrO_2 SYSTEM. (Garvie, 1968)

The existence of the compound $CaZr_4O_9$ is certainly consistent with the fact that cubic ZrO_2 stabilized with CaO is far more stable than the material stabilized with MgO in which no compound has been reported to form.

The level of stabilization of zirconia in the $CaO-ZrO_2$ system can be defined from the phase diagram shown in Figure 6. Any composition which at high temperatures lies in the two-phase (tetragonal ZrO_2 + cubic solid solution) field will only be partially stabilized on cooling. The further the composition lies from the cubic phase boundary, the greater will be the driving force for partial destabilization on cooling. On the other hand, compositions lying within the cubic field at low temperatures will be monophase on cooling and are termed "fully-stabilized". The solubility level of CaO in pure zirconia is very small. Consequently, the appearence of free zirconia in the $CaO-ZrO_2$ system will be dependent to some extent on the diffusion of Ca^{+2} from those grains which are to become pure zirconia to local cubic regions wherein the stability will be subsequently increased. This diffusion step will necessitate high temperatures and even though the driving force for pure ZrO_2 precipitation increases as the temperature is decreased, it is probably restricted by the reduced diffusion coefficients of the cations in the system.

Assuming that the cubic field is generated by a solid solution series between cubic ZrO_2 and $CaZr_4O_9$, there are two major aspects to the problem of destabilization of the cubic phase. The first is concerned with the intrinsic thermodynamic instability of the cubic phase, and may be subdivided into two secondary categories, namely precipitation of ZrO_2 from solid solution and decomposition of the cubic phase(33). Sukharevskii et al(34) offered evidence for the precipitation of ZrO_2 from solid solution by observing the decrease in the quantity of the cubic phase (ΔC) in slowly cooled specimens compared with those quenched after ignition at 1750°C. Their data are summarized in Figure 7. The amount of destabilization is a function of the degree of the supersaturation in the cubic phase. It is worth noting that these data are difficult to interpret in terms of the conventional description of the cubic phase as a solid solution of CaO in ZrO_2. If one considers ZrO_2 to be the solute dissolved in $CaZr_4O_9$, it is clear that high degrees of supersaturation can only occur at low CaO compositions, which is what is observed. Decomposition of the cubic phase according to the reaction, cubic phase = $ZrO_2 + CaZrO_3$, occurs at temperatures below ≈ 1200°C, and is therefore probably exceedingly slow(33).

The second main aspect of destabilization is concerned with chemical attack of the cubic phase by impurities, consisting of acidic oxides which combine with CaO. This mode of decomposition is best described as corrosion rather than destabilization.

Duwez et al(24) and Weber et al(35) reported that calcium-stabilized zirconia is not affected by isothermal heat treatment in the range 1600° to 2000°F after heating periods of up to 2000 hours. However, Buckley and Wilson(36) showed that the amount of cubic phase in commercial partially stabilized zirconia (4% CaO), used in a heat exchange furnace, decreased from 80% to 58% after 47 thermal cycles between 1600° and 2000°F. They pointed out that as the material used in their work was only PSZ and because maximum destabilization occurred

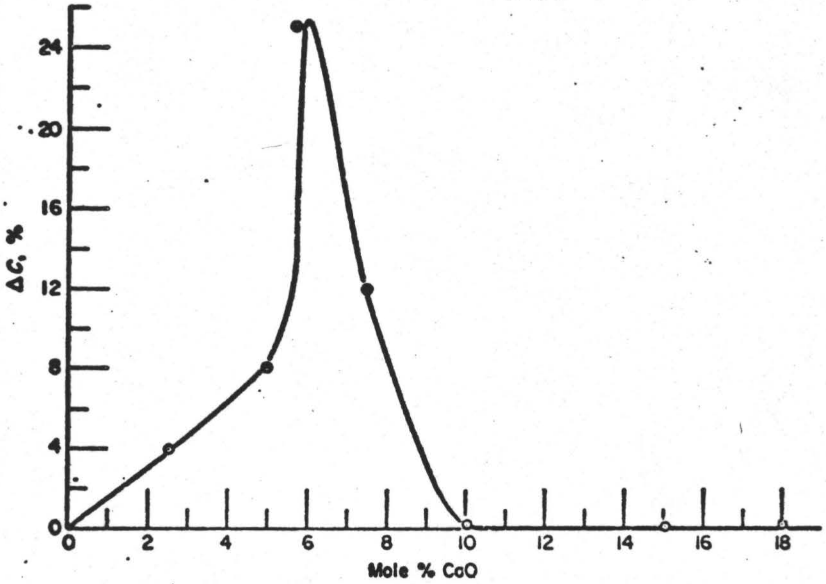

FIGURE 7- Decrease in amount of cubic phase in slowly cooled samples as a function of composition (Sukharevskii, 1961).

in the range in which monoclinic zirconia inverts to tetragonal zirconia, it appears that the cubic zirconia was destabilized by the inversion of monoclinic and tetragonal zirconia. The large volume change accompanying the inversion caused mechanical pressure to be imposed on neighbouring cubic grains. A compressive stress on cubic zirconia would favor diffusion of calcium ions from solid solution because of the relatively large size of the calcium ions. Also, they reported that a sample of completely stabilized zirconia (100% cubic) was not affected by 100 cycles in their laboratory tests.

2.3 Mechanism of the Monoclinic to Tetragonal Transformation in ZrO_2

The occurrence of a reversible transformation in pure zirconia was first reported by Ruff and Ebert(18). They carried out high-temeprature X-ray studies and showed that the room temperature monoclinic form transforms to a tetragonal structure at about 1100°C. Subsequently, the existence of this polymorphic change was inferred from dilatometric studies and length measurements. Kauer et al.(37) and Murray and Allison(38) reported that the transformation proceeds through a process of nucleation and growth which indicates a diffusion mechanism. However, recent work by Wolten(23,39) and others(40,41), has revealed that this phase transformation possesses many of the characteristics associated with diffusionless phase transformations of the type observed in several pure metals and metal alloy systems. The high temperature X-ray diffractometry data of Wolten suggest that the zirconia inversion is very similar to the Fe-Ni martensitic class of displacive transformations. Displacive transformations are described as distoritons of atoms or lattice networks in which the atomic linkages are maintained intact in their new crystal phase configuration. That is, atomic nearest neighbors do not change, in contrast to the diffusion-induced atom interchange that occurs in conventional isothermal, nucleation and growth transformations. Thus, the displacive transformation is produced by a diffusionless, shearing mechanism involving the co-operative translation of planes and/or groups of atoms or ions(42).

Martensitic transformations are divided into two general classes(43), the Fe-Ni type displaying a wide forward and reverse transformation hysteresis(44), and the Au-Cd type exhibiting a narrow hysteresis loop(45). There are important differences in the reaction behavior between the two cases.

The Fe-Ni alloys transform to martensite on cooling by the successive formation of new plates, with each one shooting out suddenly and immediately to its final size. Consequently, the course of the transformation as a function of dropping temperature is dependent upon the rate of nucleation and the size of the fully grown plates, but not upon their rate of growth. Such reactions are typified by a high degree of supercooling and hence a relatively large driving force below the martensite-start temperature. Once nucleated, each martensitic unit propagates quickly until it collides with a structural barrier or its mechanism becomes jammed. On continued cooling, there is no additional growth of the plate despite the increased driving force; further nucleation occurs elsewhere in the parent phase. Bunshah and Mehl(46) have found that the propagation rate of martensitic plates in an Fe-Ni alloy is about 10^5 cm/sec, with a time of formation of 0.05 - 0.5 µsec. This corresponds to one-third the velocity of sound.

In contrast, the Au-Cd alloys generate martensitic plates that do not reach their final size at once. Instead, although each unit seems to nucleate suddenly and "pop-out" to a detectable size within a small fraction of a second, further propagation in length and thickness continues with the decreasing temperature until collision takes place. Martensitic reactions in this category start to transform with comparatively little supercooling, and the driving force is insufficient to supply the strain-energy and other non-chemical requirements of fully grown plates. In other words, the growth of a martensitic unit may be halted at a given temperature because of the limited driving force available. As the temperature falls, the enhanced driving force permits the growth to proceed while additional nucleation also ensues. The progressive propagation is intrinsically a rapid process in that it is able to pace the dropping temperature and maintain the athermal character of the reaction. But the rate of propagation is then controlled by the rate of cooling, unlike the case for reactions of the Fe-Ni type.

Corresponding differences carry over to the reverse transformation on heating. In systems of the Au-Cd class, the reverse transformation occurs with relatively little superheating; the martensitic plates shrink more or less progressively and disappear approximately in the same reverse order of their formation. However, in the Fe-Ni case, appreciable superheating is necessary to start the reversal, and the plates do not snap back out of existance, but often transform piecewise in smaller platelike units(47).

Some metallic systems possess isothermal components, but they are generally small(48-50). In most martensitic systems, the isothermal component is either not operative or is obscured by the predominant athermal behaviour. In almost all instances the isothermal reaction proceeds by the nucleation of new plates, rather than by the growth of existing ones, and the plates reach full size within a small fraction of a second. The appearance of the martensite and its mode of formation are quite similar to those of the athermal transformation. Such isothermal reactions are obviously controlled by the rate of nucleation.

It is well known(51-53) that the M_s (martensite-start temperature on cooling) temperature can be varied by applied stress. Patel and Cohen(54) have utilized this effect to demonstrate the interaction of mechanical energy with the thermodynamics of martensitic reactions. The acting stress system is resolved into components parallel to the shear and dilatational displacements of the transformation, being respectively parallel and normal to the habit plane. The mechanical work done on or by the transforming region, as the resolved components of the acting stress are carried through the corresponding transformation strains, is added algebraically to the chemical free energy change of the reaction in order to compute the alteration in temperature at which the critical value of the driving force to start the transformation is attained. The M_s is either raised or lowered depending on whether the mechanical work aids or opposes the chemical driving force.

As mentioned earlier, the monoclinic to tetragonal phase transformation in zirconia was likened to the Fe-Ni class of martensitic transformation. Both have many characteristics in common, although the latter is accompanied by plastic deformation which is unlikely to occur to the same extent in the ceramic material. For this reason, Wolten(23) coined the phrase, "brittle-martensite" transformation to describe the zirconia inversion. According to his views, the following crystallographic orientation relationships should prevail during the transformation: the C axis in both structures should be parallel; the monoclinic b axis should remain parallel to one tetragonal a axis while the other tetragonal a axis should be inclined 9.2° to the monoclinic a axis.

Smith and Newkirk(14) reported that the conversion could take place by rotation of the triangular co-ordinated oxygen ions in the (100) planes. The crystallographic relationship between the two structures(39) is shown in Figure 8. This mechanism implies the following orientation relationships (habit planes):

$$(001)_m \parallel (001)_t$$

$$(100)_m \parallel (110)_t$$

These relations were also observed by Bailey(55). He described the transformation as a shear-type martensitic process and pointed out that the monoclinic phase formed during cooling through the transition temperature is generally twinned. He determined that the extent of twinning is much greater in completely enclosed grains, i.e., grains constrained on all sides by neighbouring ones. This phenomenon was called "transformation twinning" (by Beurger(56)). The twinning planes were defined by Bailey as (100) and (110). He reported that the shear associated with (100) twinning is in the [001] direction and

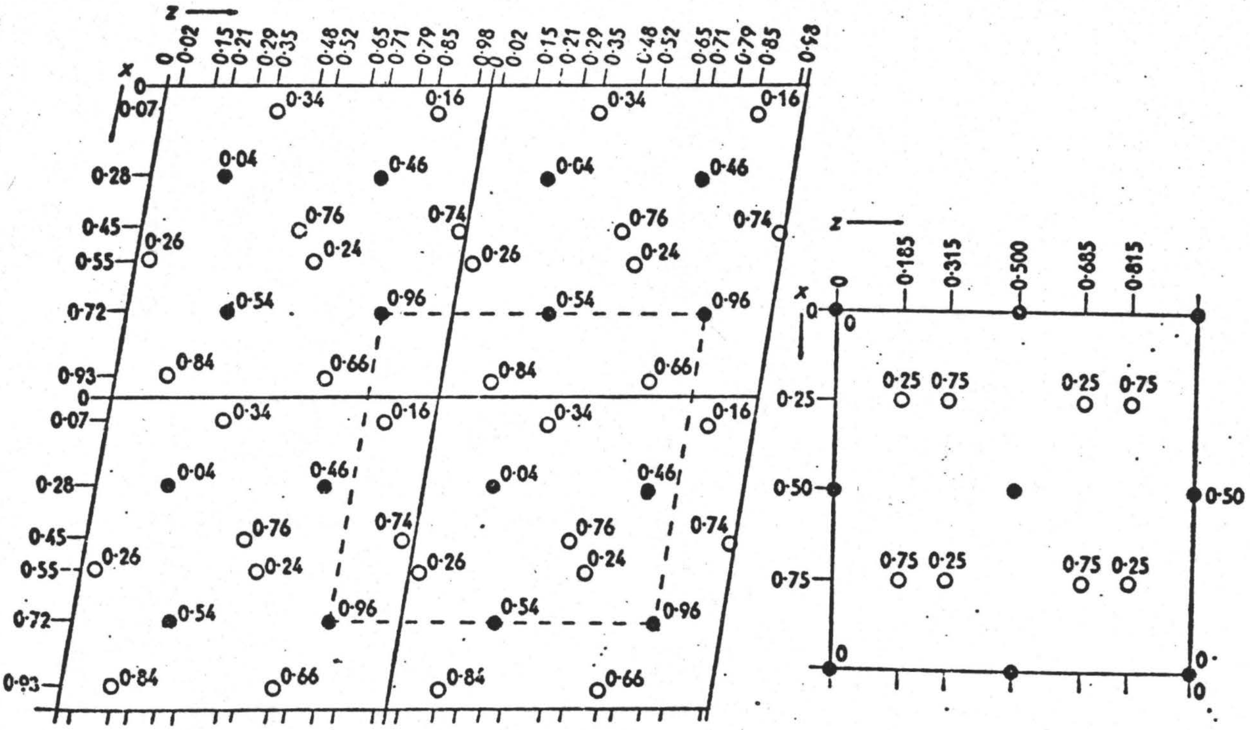

Fig. 8. Projection of ZrO_2 structure parallel to y direction onto x–z plane. Left: monoclinic. Right: Tetragonal. Parts of four monoclinic cells enclosed by broken lines become tetragonal cell after transformation. Solid circles: Zr. Open circles: O.

(Wolten, 1964)

equal to twice the transformation shear. Thus for the twinning mode about 50% of the material must be twinned. Fine twinning (0.1 μ or less) is generally observed in the martensite in the systems most extensively studied(57-59).

Grain and Garvie(60) investigated the transformation and offered an interpretation based on Ubbelohde's(61) theory of continuous phase transformations. According to this theory, whenever a crystal of monoclinic zirconia is heated to a temperature within the transition region, domains of the tetragonal phase form in the monoclinic matrix. Continuous transformations invariably occur over a temperature interval and show hysteresis. One criterion for the appearance of these phenomena is that the high and low temperature structures must be closely related so that atom movements in going from one structure to the other are small (less than an interatomic distance). When this occurs the two phases, intimately coupled, may co-exist in a hybrid single crystal, thus violating Gibb's classical phase rule, which is based on the fundamental postulate that phases in equilibrium must be distinct and separate. They reported that the transformation is associated with considerable strain energy because the domain boundaries are coherent and there is an appreciable volume difference of about 7% expansion on cooling, between the two phases; thus, a strain energy term must be added to the free-energy description of the system, thereby allowing an additional degree of freedom; the phase rule violation is then only apparent. The strain energy arising from the co-existance of both phases brings the reaction to a halt at any given temperature within the transition region; to bring about any further change in the amount transformed, the temperature must be changed. The strain involved in accommodating a monoclinic domain in a tetragonal matrix is not the same as the strain arising from a tetragonal domain in a monoclinic matrix. This situation would give rise to hysteresis as shown in Figure 9, which is a main characteristic of the transformation. Grain and Garvie reported that this athermal kinetic behaviour depends upon the crystal size of the sample studied; samples of crystallite size less than a domain size ($\sim$ 1000 Å) displayed classical kinetics. Figure 10 shows the usual athermal kinetics obtained with well crystallized zirconia. The reaction, at any given temperature, is time independent. Figure 11 shows the rate of transformation for finely divided zirconia (less than 1000 Å); the rate now is time dependent, and obeys the following equation:

$$q = K \log (1+t) + b$$

where q = the fraction of monoclinic phase transformed

t = time, and

K,b = constants.

They found that the rate constant is a linear reciprocal function of the crystallite size and it becomes zero when the crystallite size is about 1150 Å so that the domain size is of the order of 10^{-5} cm.

Recently Bansal and Heuer$^{(62)}$ studied the monoclinc to tetragonal transformation in ZrO_2 single crystals and polycrystals in both the forward and reverse directions and found it to be martensitic with large temperature hysteresis. They reported that surface relief

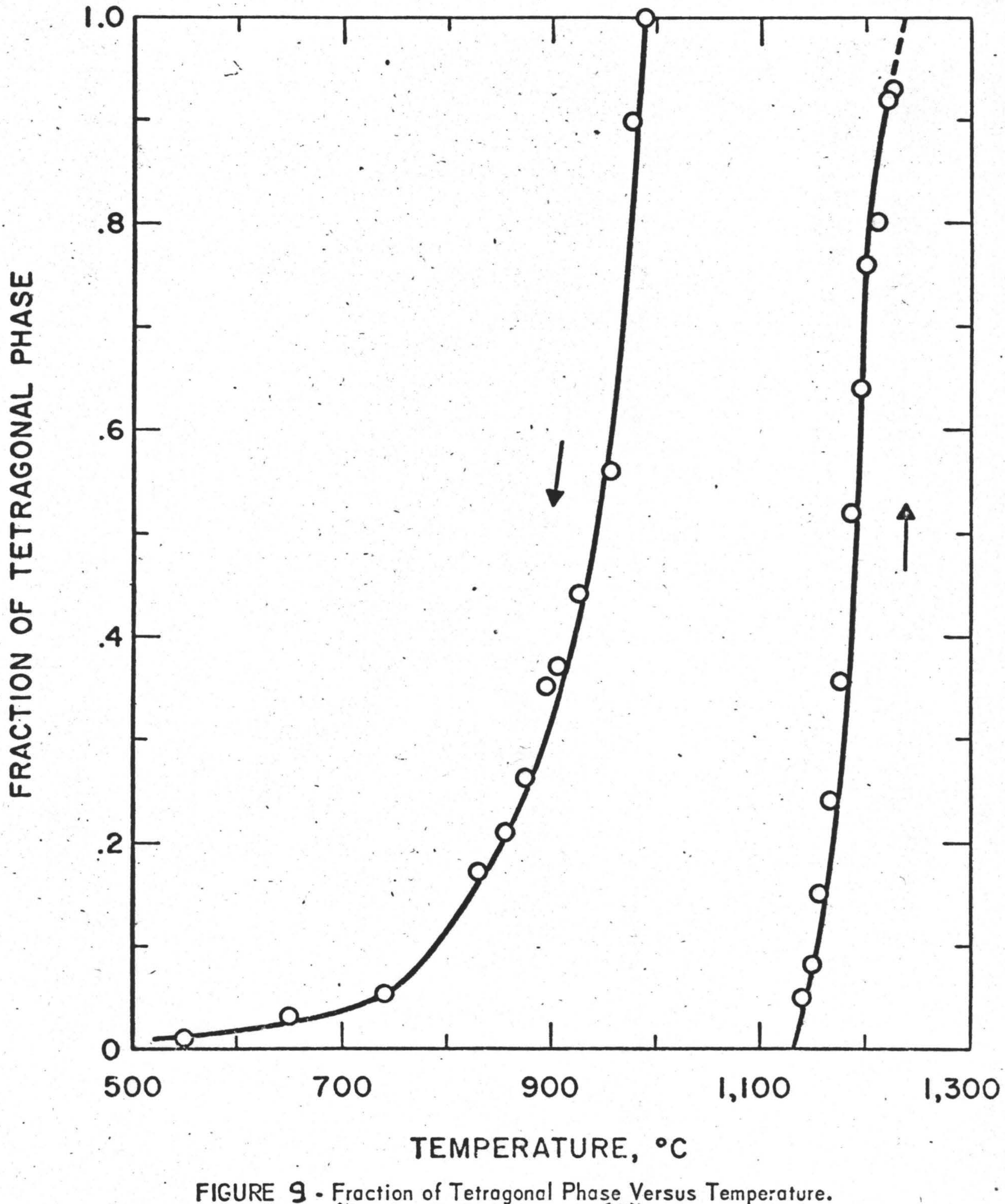

FIGURE 9 - Fraction of Tetragonal Phase Versus Temperature.
(Grain & Garvie, 1965)

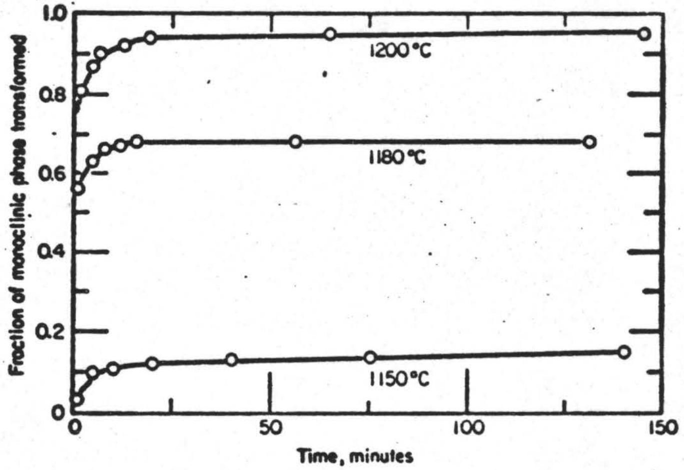

FIGURE 10 Fraction of monoclinic phase transformed versus time; sample preheated 1500°C (Grain and Garvie, 1965).

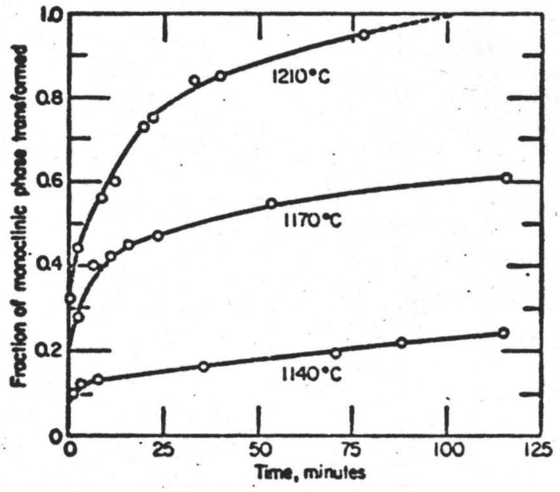

FIGURE 11 Fraction of monoclinic phase versus time; sample preheated 900°C (Grain and Garvie, 1965).

accompanied the transformation in both directions. Their high-temperature metallographic study established the athermal, diffusionless and shear-type nature of the transformation. The habit plane has been determined and found to be (010). They indicated that the lattice invariant shear occurs by slip in the high temperature tetragonal phase and not by twinning in the low-temperature monoclinic phase. However, deformation twins have been observed, suggesting that they arise from accommodation stresses generated during the transformation.

The martensitic phase transformation of monoclinic-tetragonal zirconia is highly pressure sensitive(63-67). Dow Whitney(63) has determined the pressure-temperature (P-T) diagram for the phase transformation and this is shown in Figure 12. He calculated the slope of the theoretical equilibrium line between the two phases as $- 3.02 \times 10^{-2}$ degree/bar and verified his calculations with electrical resistance measurements up to 15 Kbars(64). Vahldiek et al.(65) found that quenching from 15 to 20 Kbars and 1200° to 1600°C resulted in a mixture of monoclinic and tetragonal phases. They also found, however, that rapid decompression from pressures as high as 90 Kbars at room temperature will not retain any of the tetragonal phase. With respect to the sub-transformation temperature occurrence of the monoclinic-tetragonal phase transformation, three possible sources of this phenomenon will be considered, namely grain size, existence of non-equilibrium structure and the existence of internal stresses.

Garvie(68) reported that the metastable tetragonal phase may be obtained at room temperature if the crystallites are small (less than 300 Å). However, recent work by Maiti et al.(69) showed that for very

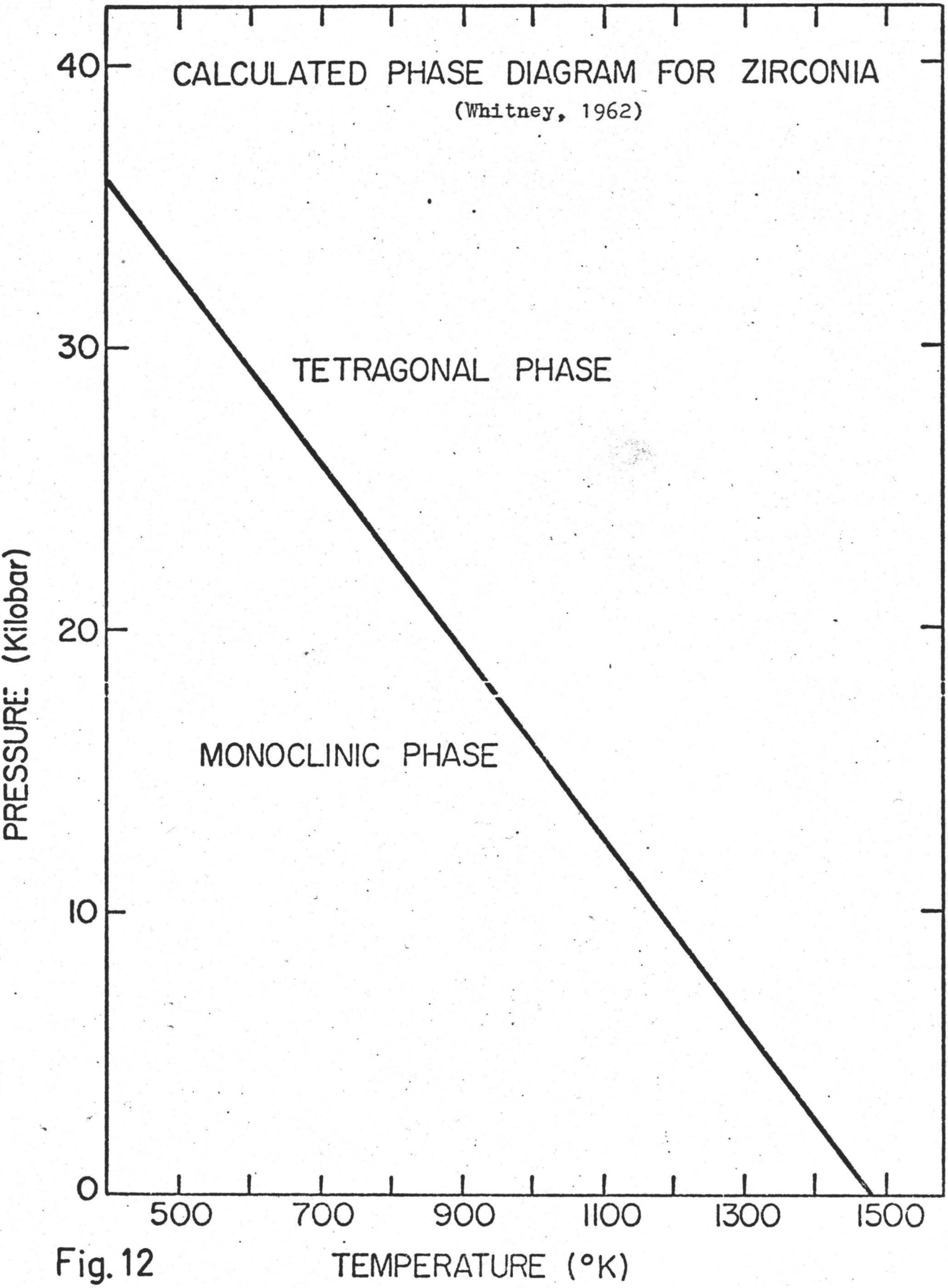

CALCULATED PHASE DIAGRAM FOR ZIRCONIA
(Whitney, 1962)

Fig. 12

fine crystallites the transformation temperature on heating was not influenced by the particle size whereas that on cooling was shifted to lower values (850° - 1000°C) depending on the history of the specimen and the experimental variables. Therefore, as the transformation was observed at lower temperatures on heating PSZ, it would appear that the grain size is not responsible for the PSZ observation.

Considering the existence of internal stresses, Green(70) carried out dilatometric experiments to determine the transformation temperature on heating for the two different batches of CaO-PSZ used in this study. An example of his results is shown in Figure 13. Normally, the transformation starts at about 1100°C. The first batch (#1), prepared by very slow cooling from the fabrication temperature, gave a transformation start temperature $\approx$ 890°C. However, the second batch (#2), which was prepared by quenching from the fabrication temperature, gave values of $\approx$ 950°C. He calculated the maximum internal stresses in both, based on the Dow Whitney slope and reported a value of 40,000 psi in batch No. 1 and 20,000 psi in batch No. 2. Material No. 1 should have a structure closer to the equilibrium one than material No. 2 because of the extended cooling cycle. The depression of the transformation temperature and internal stress data indicate the reverse, however, based on normal kinetic considerations. Consequently, it would appear that non-equilibrium conditions do not account for the ΔT_{trans} depression in CaO-PSZ.

It seems, therefore, that the major influence on the transformation temperature is probably due to the presence of internal stresses within the material. In other words, the existence of the internal stresses may cause the transformation to occur at subtransition temperatures in keeping with the P-T relationship of Dow Whitney(63).

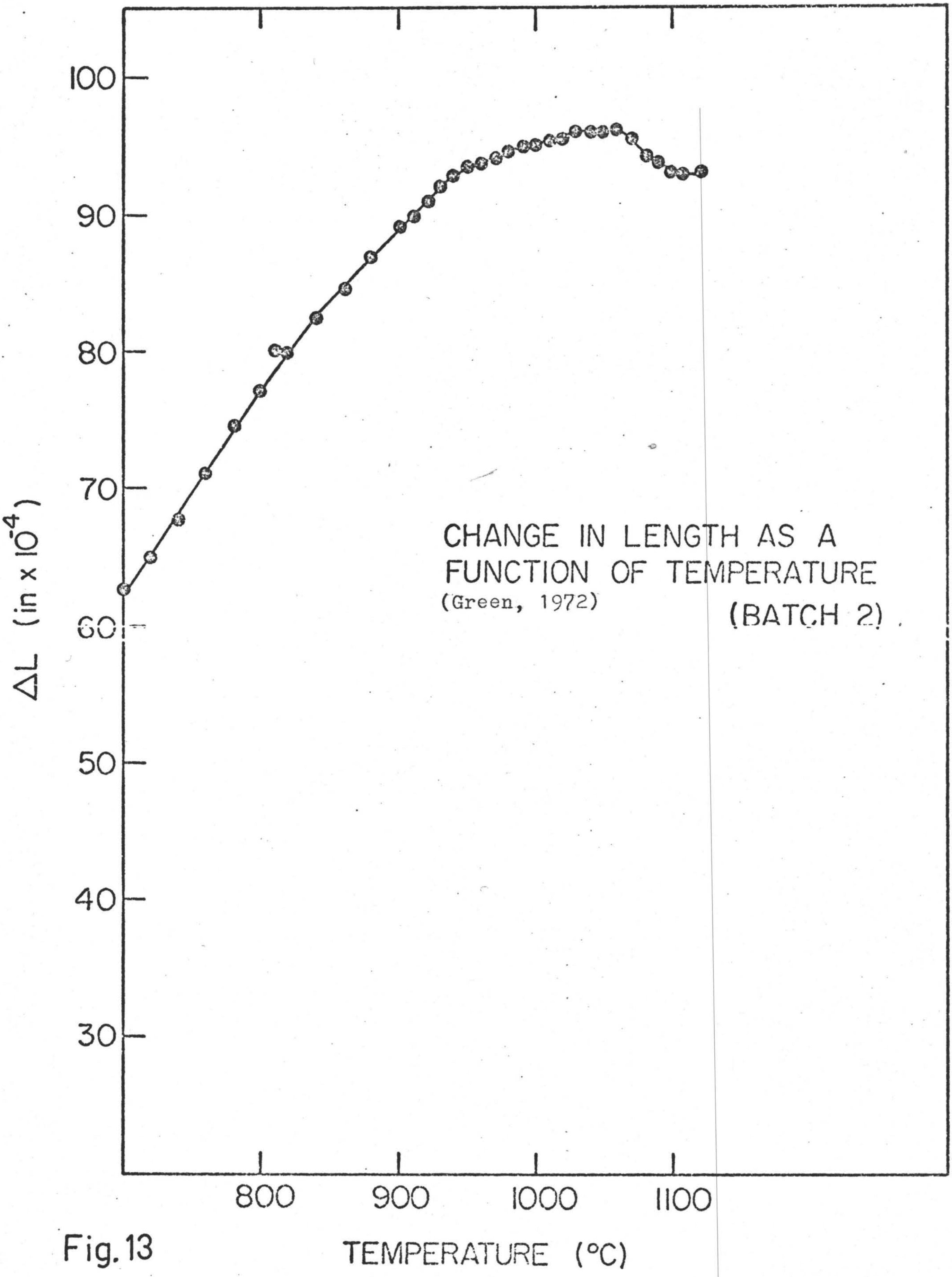

CHANGE IN LENGTH AS A FUNCTION OF TEMPERATURE
(Green, 1972)
(BATCH 2)

Fig. 13

2.4 Thermal Shock Resistance

The susceptibility of ceramic materials to thermal stresses has been recognized for a long time. More than one hundred years ago equations for the thermal stresses arising from temperature gradients in a cylinder were derived by Duhamel(71). Since that time, efforts have been made to determine quantitatively the thermal shock resistance of ceramic materials.

At the present time, thermal stress resistance of brittle ceramics can be defined in two ways. The first approach is based on thermoelastic theory(72). Material properties are selected such as to avoid the initiation of fracture by the thermal stresses. In general, this requires materials with high values of tensile strength, thermal conductivity, and thermal diffusivity combined with low values of thermal expansion, Young's modulus of elasticity and Poisson's ratio(73). For the rapid relaxation of thermal stresses by creep, low values of viscosity also are desireable(74,75).

The second approach ignores the question of fracture initiation(76), and is concerned with the extent of crack propagation and the resulting change in physical behaviour of the material. For instance, thermal stress resistance may be determined by the relative change in strength, the loss of weight, or the change in permeability of a grossly shocked body. Hasselman(77) has suggested that the extent of crack propagation in thermal stress fracture is proportional to the elastic stored energy of fracture and inversely proportional to the surface fracture energy required to create the new crack surfaces. On this basis, he suggested that superior materials should have high values of the "thermal stress damage resistance parameter", defined as:

$$R = E\gamma/S_t^2\,(1-\nu) \qquad (1)$$

where E is Young's modulus, γ is the surface fracture energy, S_t is the tensile strength and ν is Poisson's ratio. It is of interest to note that high values of R require high values of Young's modulus and low values of tensile strength, in contrast with the requirements to avoid the initiation of thermal stress fracture. Nakayama and Ishizuka(78) investigated the validity of this parameter. For a variety of materials they found a positive correlation of R and thermal shock behaviour as determined by the number of cycles required to produce a given percentage loss of weight. They also found a negative correlation between thermal shock resistance and the parameters which determine the resistance of thermal stress fracture initiation.

More recently, thermal stress crack stability and propagation has been analyzed by Hasselman(79), using a fracture mechanical approach which followed Berry's(80) analysis of crack propagation under constant deformation conditions. The theory was discussed with emphasis on crack propagation behaviour in severe thermal environments in which thermal stress fracture initiation cannot be avoided. Hasselman demonstrated that the critical temperature difference required for crack instability is given by:

$$\Delta T_c = (2G/\pi \ell \alpha^2 E)^{1/2}(1+2\pi N \ell^2) \qquad (2)$$

where N is the crack density (cracks/unit area) and ℓ is the crack half-length. When this function is plotted as a function of ℓ (at constant values of N) it is concave upwards, passing through a minimum. ΔT_c is a function of N at long crack lengths only. This can be shown by approximating ΔT_c (equation 2) for short and long crack lengths. For short crack length, $2\pi N \ell^2 << 1$;

$$\Delta T_c \approx (2G/\pi \ell \alpha^2 E)^{1/2} \qquad (3)$$

which is independent of N. For long crack length, $2\pi N \ell^2 >> 1$;

$$\Delta T_c \approx (8\pi G N^2 \ell^3/\alpha^2 E)^{1/2} \qquad (4)$$

i.e., ΔT_c to be directly proportional to N. For short crack lengths, the slope is negative so that there is always more than enough stored elastic energy to drive the cracks. When ΔT_c is reached, cracks propagate with high valocity, resulting in a sudden, catastrophic loss in strength. For long crack lengths (to the right of the minimum) the slope is positive. This implies that when the crack denisty and length attain values which satisfy a given ΔT_c, no further crack propagation occurs. The degree of undercooling must consequently be increased to continue driving the crack. This region was termed by Hasselman that of "quasi-static" propagation and is desireable in high temperature materials as no sudden catastrophic loss in strength occurs.

As mentioned earlier, the poor thermal shock resistance of pure zirconia is attributed to the volume change associated with its phase transformation. On the other hand, the high thermal expansion together with the very low thermal conductivity are mainly responsible for the poor thermal shock resistance of the "fully stabilized material". Curtis(81) first reported that improved thermal shock behaviour could be obtained by adding a proportion of monoclinic zirconia to the cubic form to make a "partially-stabilized" body. It was originally thought that this lowered the thermal expansion, while the effect of the phase change was not sufficient to cause failure. However, recent workers(2) have reported that the presence of two phases and the phase change itself may play a considerably more important role in the improvement of the thermal shock resistance of this material. They reported that thermal stresses can be relieved through the production of extensive microcracking. Due to their large numbers, these cracks propagate quasi-statically and the material maintains a large portion of its strength even after continuous thermal cycling.

A stress relief model based on stress induction of the phase transformation in PSZ has been developed(4). According to this model, the transformation of the fine monoclinic domains in the PSZ can be "tripped" at a certain value of total stress within the system. This total stress, σ_t, is composed of two components, namely the internal stress in the system as a result of fabrication, σ_i, and the stress induced in the material as a result of the thermal shock. This model will be discussed later in more detail. Evidence for the existence of such internal stresses was obtained by Jaeger and Nickel(82) in the MgO-PSZ system. On conducting thermal expansion measurements they noted a contraction between 800° and 900°C as well as the usual contraction above 1080°C associated with the monoclinic-tetragonal transformation. The lower temperature contraction, they concluded, is probably associated with the domain ZrO_2 transformation.

Strong evidence for the triggering of the phase transformation at sub-transition temperatures was obtained by the studying of the phenomenon of "ratchetting". Ratchetting is the progressive increase in length of thermally shocked bars. Bansal and Heuer(83) examined the microstructure of monoclinic ZrO_2 thermally cycled above the transformation temperature and observed much grain separation to occur. This was accompanied by a volume expansion due to the transformation and this expansion was termed "ratchetting". Ratchetting experiments on carefully chosen compositions of CaO-PSZ were carried out(4), and some of these data are shown in Figure 14. The data falls into two categories, those obtained in and above the transition region and those obtained below it. Above the transformation temperature, each cycle shows an increase in length because of the disruptive effect of the inversion which must occur during each cycle. For sub-transformation temperatures, however, a steady state condition was reached after the first few cycles. That ratchetting takes place at sub-transformation temperatures is further evidence for the occurrence of the phase transformation at these temperatures. That it ceases after the first few cycles indicates the role of stress in triggering the transformation. As previously mentioned

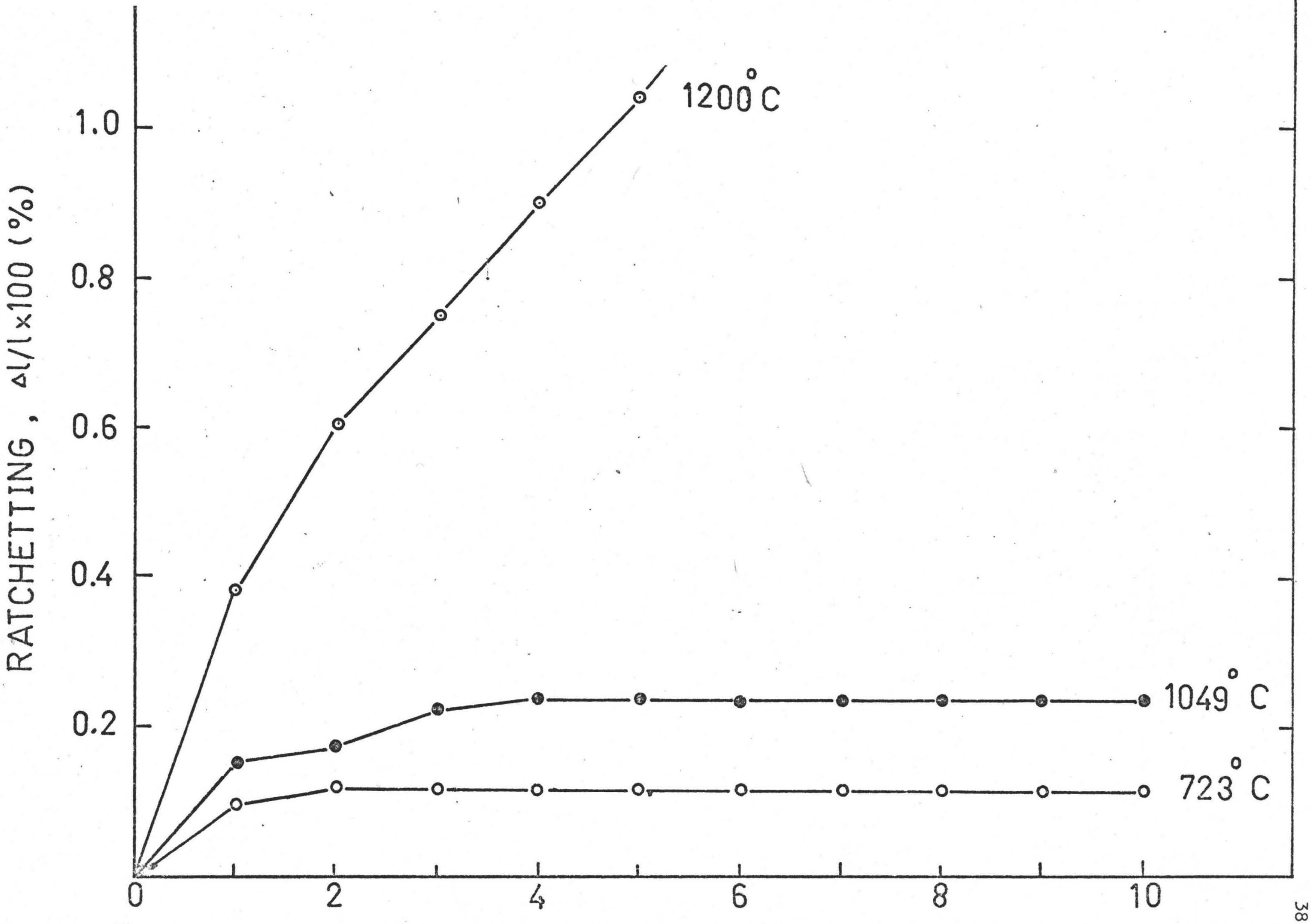

Fig. 14

(Garvie & Nicholson, 1972)

the stress acting on a monoclinic domain in thermal shock probably consists of two components, the internal stress due to fabrication (σ_i) and the thermal shock stress (σ_s). A critical value of the total stress is required to trip the transformation of the domain at a given sub-transformation temperature. For a given σ_i, therefore, more domains will be tripped, the greater the ΔT_{shock}. The volume change associated with the transformation would, following the first few cycles, tend to "free" the transforming zirconia domains from the surrounding matrix. If this occurs, the level of the internal stress, σ_i, in the domain will drop, possibly below a value necessary to trip the transformation when combined with the thermal stress. In this case, no further transformation would occur during the subsequent cycles and the ratchetting would cease.

The main purpose of this work was to further elucidate the mechanism which is responsible for the relief of stresses produced during thermal shocking of CaO-PSZ. The major region of thermal shock will always be the outer surfaces of the shocked sample. Therefore, it was decided to use a surface replication technique to follow the structural changes from thermal shock.

CHAPTER III

EXPERIMENTAL WORK

3.1 Material Preparation

Two different batches of calcia PSZ were studied. The two batches were subjected to different heat treatments during fabrication. The specimens were made from Tizon C.P. zirconia (99.7) micronized grade and calcium oxide reagent powders. The amount of CaO in the specimens was about 3.4% by weight. Bars of 2 7/8 x 3/8 x 3/4 in. were isostatically pressed at 22,000 psi, fired for 5 hours at 1850°C and then cooled to room temperature. The different heat treatments of batches #1 and #2 involved the rate of cooling after the firing stage. Batch #1 was slowly cooled with an extended anneal at 1300°C, while batch #2 was fast cooled to room temperature. The specimens obtained were two phase mixtures of monoclinic and cubic zirconia.

3.2 Experimental Work Procedure

3.2.1 Optical and Scanning Electron Microscopy Examinations

Efforts were made to obtain information on the microstructure of CaO-PSZ using an optical microscope. Polished samples (1 x 1/2 x 1/2 in.) were etched in a mixture of 10% Hf, 45% HNO_3 and 45% H_2O for 5 seconds and examined with a Carl Zeiss optical microscope. It was found that damage associated with the polishing process precluded any meaningful analysis. Therefore, it was decided to examine the microstructure with a scanning electron microscope.

Portions of fractured PSZ samples were mounted on aluminum holder and the surfaces coated with thin film of evaporated aluminum and examined in the S.E.M. in the usual manner.

3.2.2 Preparation of Thin Foils Using an Ion-Bombardment Technique

The main effort in this area has been directed at obtaining transmission electron microscope specimens of PSZ. Unfortunately, little success accompanied these efforts so the technique is only briefly outlined. Dr. A. Heuer of Case Western Reserve University thinned some of the material using a commercial ion thinner and the micrographs he obtained are included in this work.

Geological thin sections were made of the material and pieces mounted in 3 mm nickel grids. These grids were then located in a special aluminum holder which held eight samples in all. A schematic of the ion-bombardment apparatus is shown in Figure 15. The upper cathode (the aluminum sample holder) is connected to a copper rod and so to the power supply system. A lower anode disc, made of aluminum is connected to the ground. The power supply system and meters indicating voltage, total current and current lost from the top of the cathode complete the circuit. Argon of commercial purity (99.99%) was used as the inert gas for the discharge between the anode and cathode.

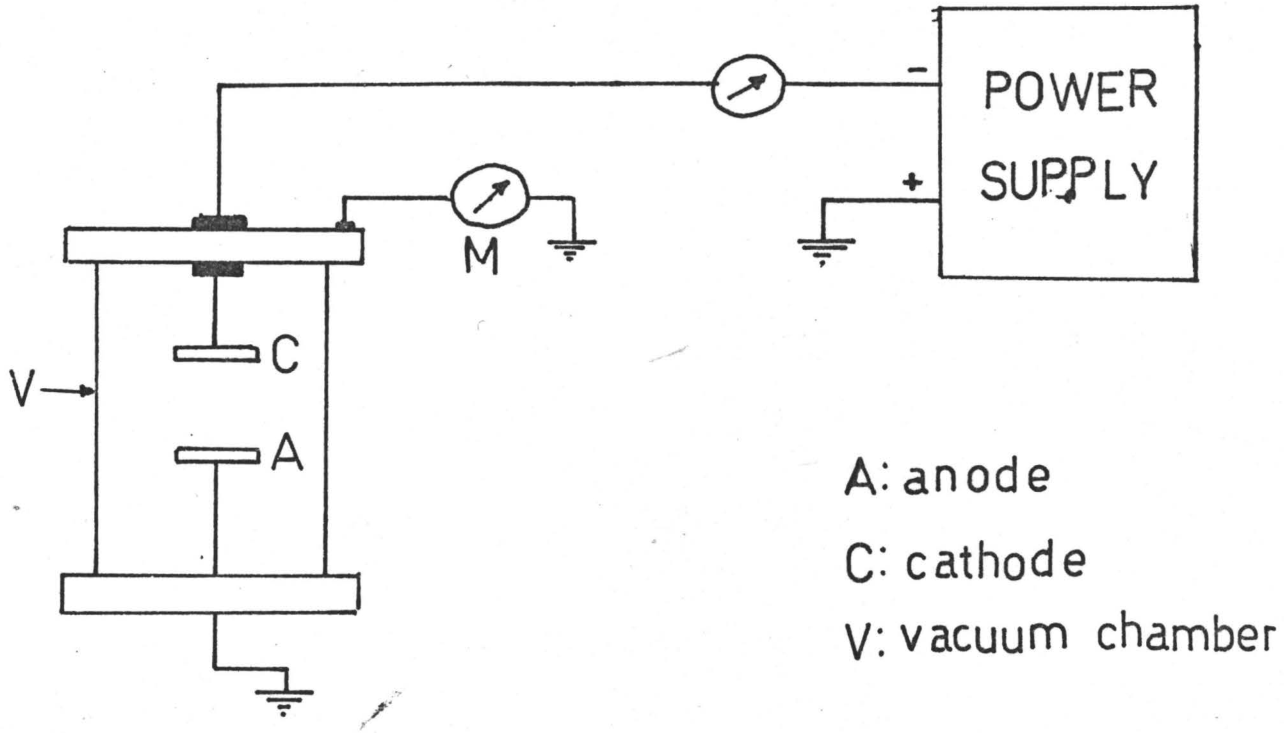

FIG. 15

A schematic diagram of the ion-bombardment apparatus used.

3.2.3 Thermal Shock Experiments

Seven bars of each CaO-PSZ batch (3 × 3/4 × 1/2 in.) were polished to 0.3 micron. γ-alumina and diamond hardness indentations were made in a square array at one end of each bar. These indentations were used to locate a region for replication.

Two-stage replicas were taken from the polished surface of each bar at room temperature and following thermal shock. The replication technique used is summarised as follows:

(i) The specified surface was covered with a solution film of coloidon in iso-amyl acetate (15%) and left to dry for 6 to 8 hours.

(ii) The dried film was stripped from the surface so as to leave it undamaged using a fine pair of tweezers. This stripping was done as soon as possible after the film had adequately dried and hardened.

(iii) The stripped film was fixed on a glass microscope slide with scotch tape, located in an evaporator and covered with a palladium layer ≈ 50 Å thick followed by a carbon layer ≈ 100 Å thick.

(iv) The replica was removed from the evaporator, cut into discs ∿ 3mm diameter and placed on a single copper grid (300 mesh). A solution of iso-amyl acetate (5 cm^3) was then added to dissolve the plastic material and the contents left to dry for 15 hours. The dried replica samples were examined under a Philips electron microscope.

The seven bars were thermally shocked from 700, 800, 900, 1000, 1100, 1200 and 1300°C to room temperature, by heating for one hour at the requisite temperature in a muffle furnace, and then removing and holding in a blast of cold air for another ten minutes. Following each cycle a further replica was taken from the same position on each bar. Each bar was subjected to ten cycles in all and the replication technique repeated following each cycle.

Other polished samples (1 1/2 x 1 x 1/2 in.) were shocked into cold water from 500, 600 and 700°C to room temperature for 2 cycles. A series of replicas were taken from the same position on the surface of each sample following the same procedure.

In addition, polished samples of batch #2 (1 1/2 x 1 x 1/2 in.) were shocked from 1000 and 1100°C into liquid nitrogen for 4 cycles and the replication technique repeated following each cycle. Also, a polished bar (3 x 3/4 x 1/2 in.) was cut into two sections and a replica taken from each half. Both portions of the bar were then placed in a furnace at 900°C and shocked for three cycles into a blast of cold air. Subsequently one-half of the bar was cycled following the regular cycle of one hour at temperature and then quenched into air for a total of ten shocks. The other half of the bar was held at temperature for the whole annealing time, i.e., 7 hours. Following both treatments replicas were taken from each half and examined in the electron microscope. The twin density on the replicas was measured using linear intercept measurements on randomly oriented test lines. More than ten lines were used for each measurement.

3.2.4 Annealing Experiments

A polished bar of each batch (3 x 3/4 x 1/4 in.) of PSZ was cut into two sections and a replica taken from each half. One portion of the bar was then placed in a muffle furnace at 1300°C and the other portion in a furnace at 900°C. Both portions were held at these temperatures for one week and then slowly furnace cooled. Following this treatment replicas were taken from each half and compared with those taken before annealing.

3.2.5 Metal Shadowing

Replicas taken from batch #2 samples thermally shocked from 800, 1000 and 1300°C into a blast of cold air for five cycles were carefully shadowed from a definite direction using palladium in order to investigate the surface relief of each sample as indicated by the replicas.

Of the various noble metals, palladium has been found the most feasible and is now routinely employed when shadowing for the best results(84).

3.2.6 Density Measurements

Samples of PSZ (1/2 x 1/4 x 1/2 in.) were cut from the bars previously thermally shocked into a blast of cold air from all the temperatures. Each sample was then weighed in air and in water, using a microbalance of a high accuracy (0.001 gm). Samples were also immersed in a scale tube (1.0 cm. internal diameter) containing water. The readings of water level were taken before and after immersion of the sample using a cathetometer (accuracy ≈ 0.001 cm). Three samples were used for each experiment. The volume of a sample was determined by displacement and from the difference in readings recorded in the immersion tube. The density of the samples was determined as a function of the number of thermal shock cycles.

CHAPTER IV

RESULTS AND DISCUSSION

4.1 Microstructure

The S.E.M. microstructure of CaO-PSZ is shown in Figure 16. The structure is bimodal and X-ray dispersion analysis indicates that the grain boundary phase (10 μ) is pure zirconia. The large grains (60 μ) appear to have an internal structure.

King and Javorsky(5) optically observed all the monoclinic zirconia phase to disappear at ≈ 2.82 % MgO in the MgO-ZrO_2 system; however, their X-ray analysis showed that at this composition, 68% by volume was still monoclinic. They also observed that the larger matrix grains appeared isotropic on petrographic examination. They therefore speculated that a cubic and monoclinic mixture is present together within the grains which act in a gross mechanical sense as a single phase. According to them, these grains are probably composed of mixed crystals of alternating cubic and monoclinic domains with a regular structural relation between them. Polishing removes the grain boundary phase in calcia PSZ so it might be assumed that King and Javorsky were observing the equivalent of the large grains reported in this work.

A transmission electron micrograph of calcia-PSZ is shown in Figure 17, which confirms the presence of a two-phase mixture in the material.

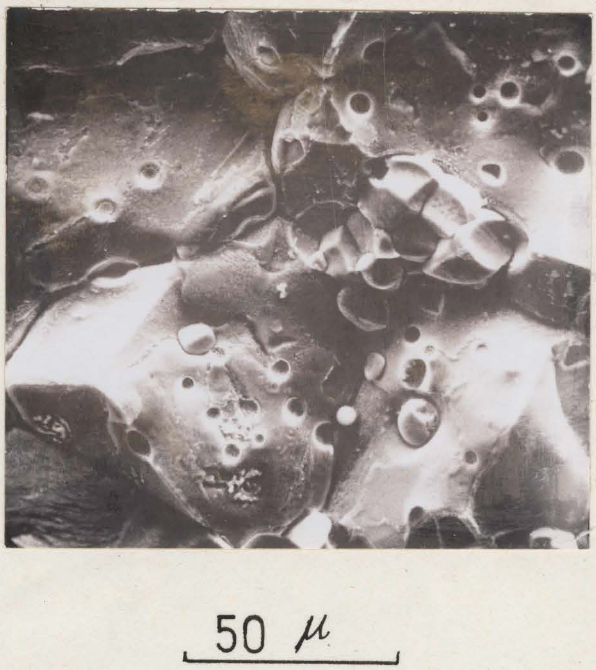

Figure 16. Scanning electron micrograph of CaO-PSZ.

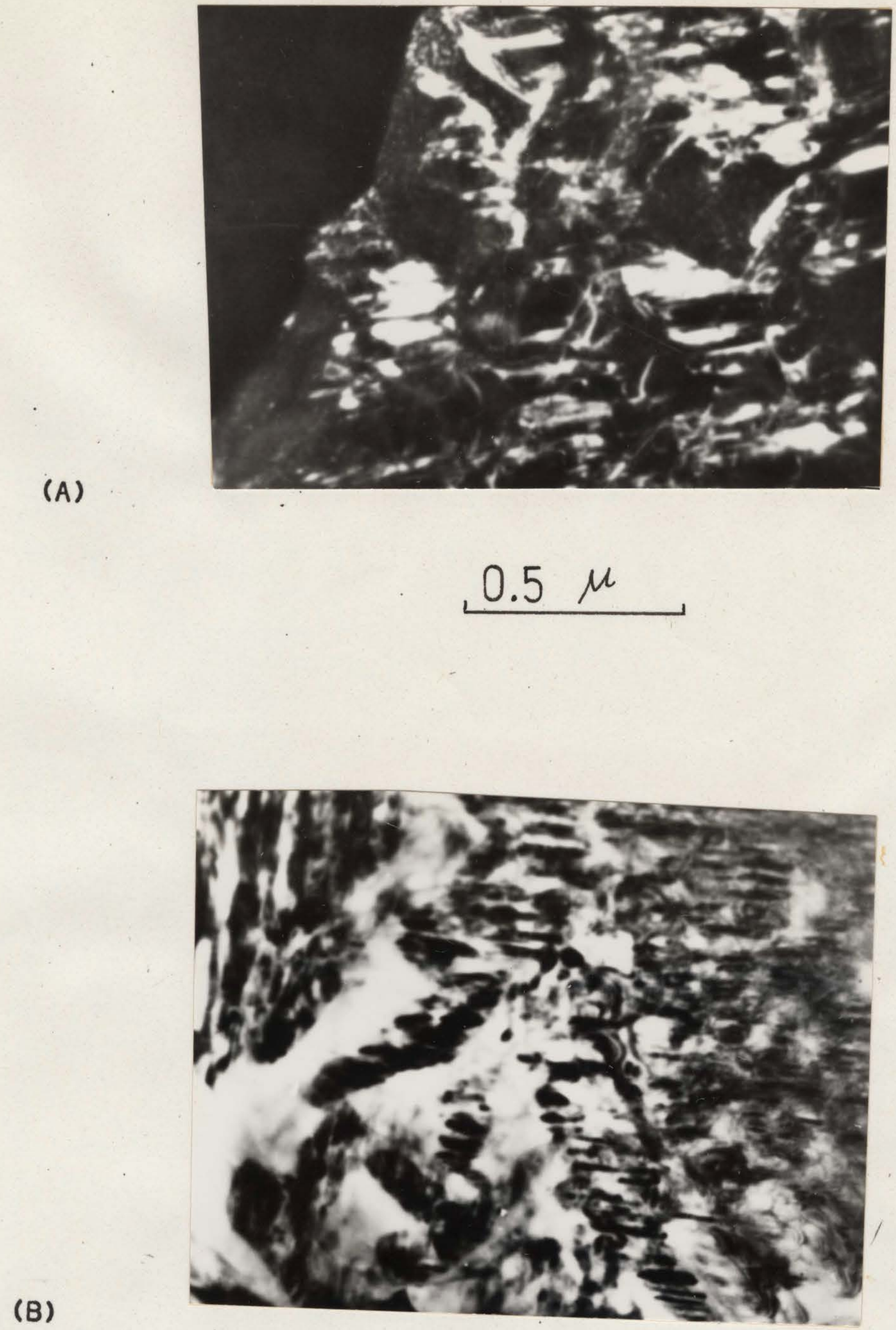

Figure 17. Transmission electron micrographs of PSZ.

Owing to the polishing step involved in foil preparation it is again assumed that this structure is that of a large grain. The monoclinic regions are heavily distorted and contain fine twins. These electron-micrographs were kindly taken by Dr. Heuer of Case Western Reserve University and were produced by ion-thinning foils of PSZ. Electron diffraction indicated that this complex structure is a two phase mixture of cubic stabilised zirconia and monoclinic pure zirconia as shown in Figure 18. The ionic conductivity of this material observed by Kontopoulos and Nicholson(85) suggests that the cubic phase is continuous in the material.

The occurrence of such a substructure can be explained by the nature of the cubic phase field in the CaO-ZrO_2 system. Garvie(31) reported that the field may be looked upon as a solid solution series between pure zirconia and the cubic compound $CaZr_4O_9$. The supersaturation of the cubic material with pure zirconia as a result of cooling from the firing temperature could lead to grain boundary precipitation of ZrO_2 followed later at lower temperatures by intragranular ZrO_2 precipitation on a fine scale in what were wholly cubic grains. King and Javorsky estimated the stress sustained by the cubic phase on transformation of the pure zirconia to be about 400,000 psi. This stress, they point out, exceeds the yield stress of the matrix at the transformation temperature and the material therefore yields. According to them, if zirconia did not have this capability for stress relief by means of a deformational mechanism, the grains would have fractured. Hart and Chaklader(7) observed superplasticity in pure zirconia during the inversion and it was suggested that the superplasticity of the monoclinic domains in the monoclinic-cubic hybrid phase is responsible for the stress relief

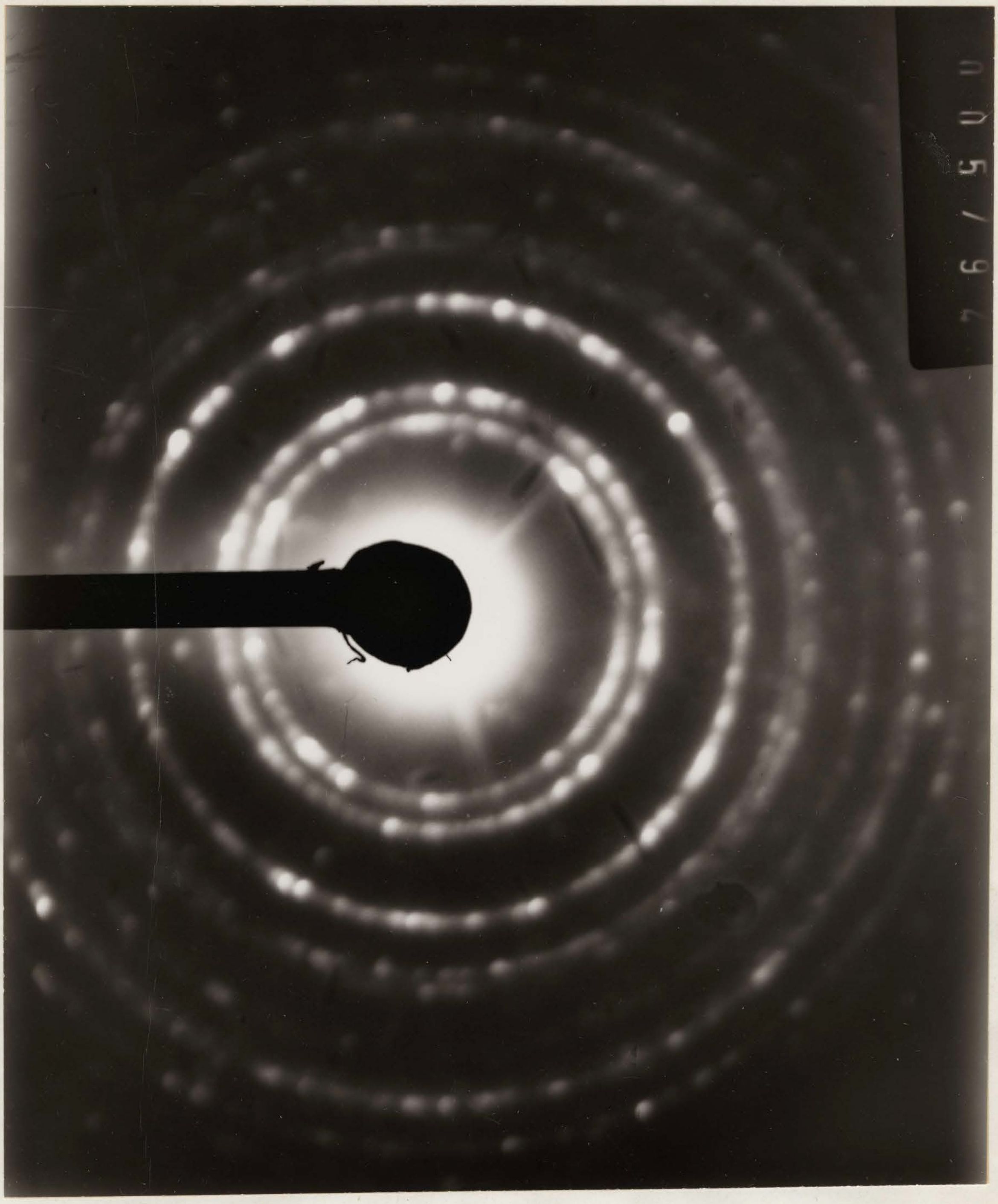

Figure 18. Diffraction pattern of PSZ sample.

mechanism observed by King and Javorsky. On the other hand, later workers reported, based on microhardness data, that the cubic phase is hardened by the stabiliser.

It is believed that the internal subgrain structure of calcia-PSZ is responsible for stress relief in this material.

4.2 Thermal Shock Behaviour of CaO-PSZ

4.2.1 Batch #2

Surface replicas obtained from all the samples were examined with an electron microscope at different magnifications. A room temperature replica from batch #2 is shown in Figure 19. Little detail is observed although some fine features (∿ 0.1 μ size) are in evidence. To investigate whether these are, in fact, surface features or replica artifacts such as dust or bubbles, a series of replicas were taken from the same surface and the first and last such replicas were compared. The results are shown in Figure 20. It can be seen that there is little change in appearance indicating that they are surface features.

All the replicas taken from samples following thermal shock indicated surface roughening. Some of these replicas from samples shocked from different temperatures into blasts of cold air, water and liquid nitrogen for different numbers of cycles are shown in Figures 21 to 27.

Large features were observed on all the replicas when examined at high magnifications and they appear to contain an internal structure.

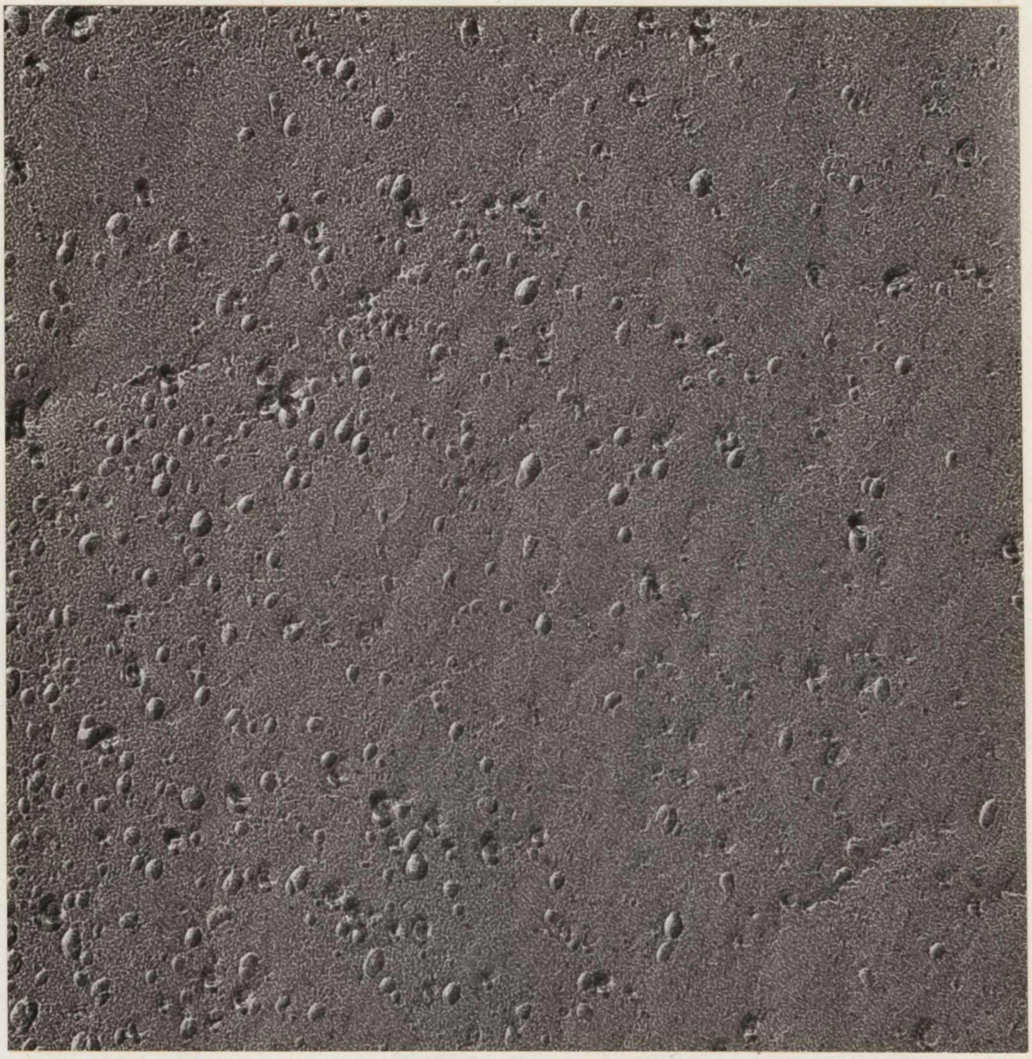

1 μ

Figure 19. Replica of polished PSZ surface at room temperature (batch #2).

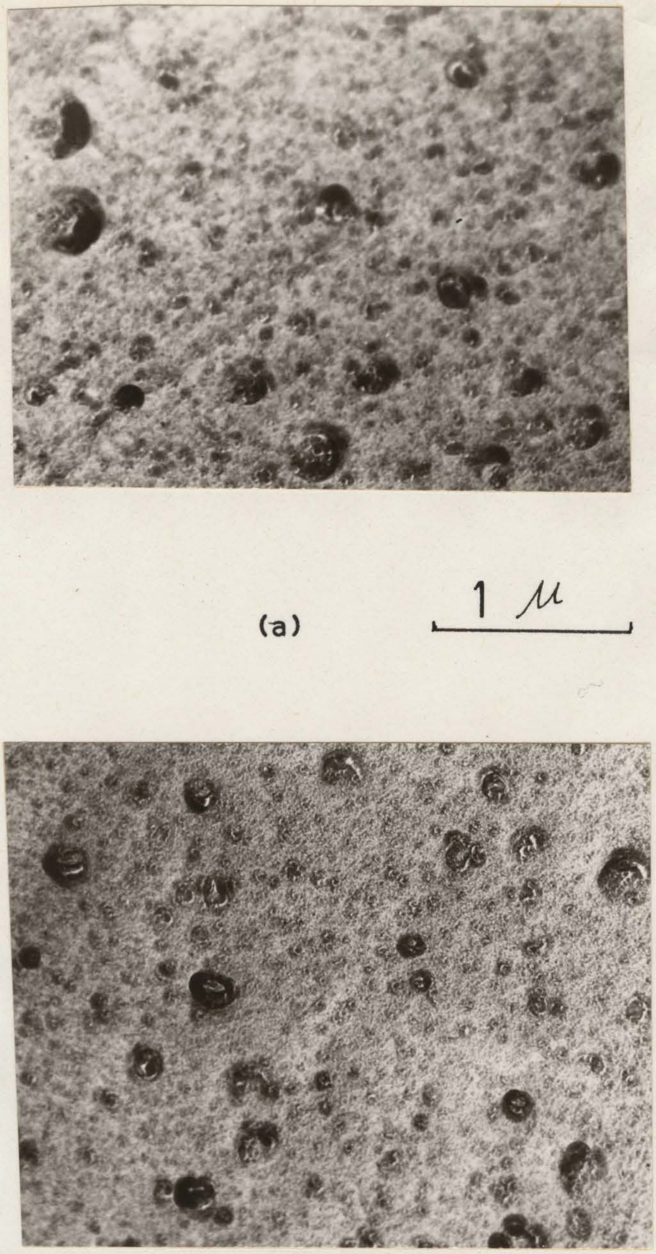

Figure 20. Replica of polished PSZ surface at room temperature for (a) unclean and (b) clean surface, batch #2.

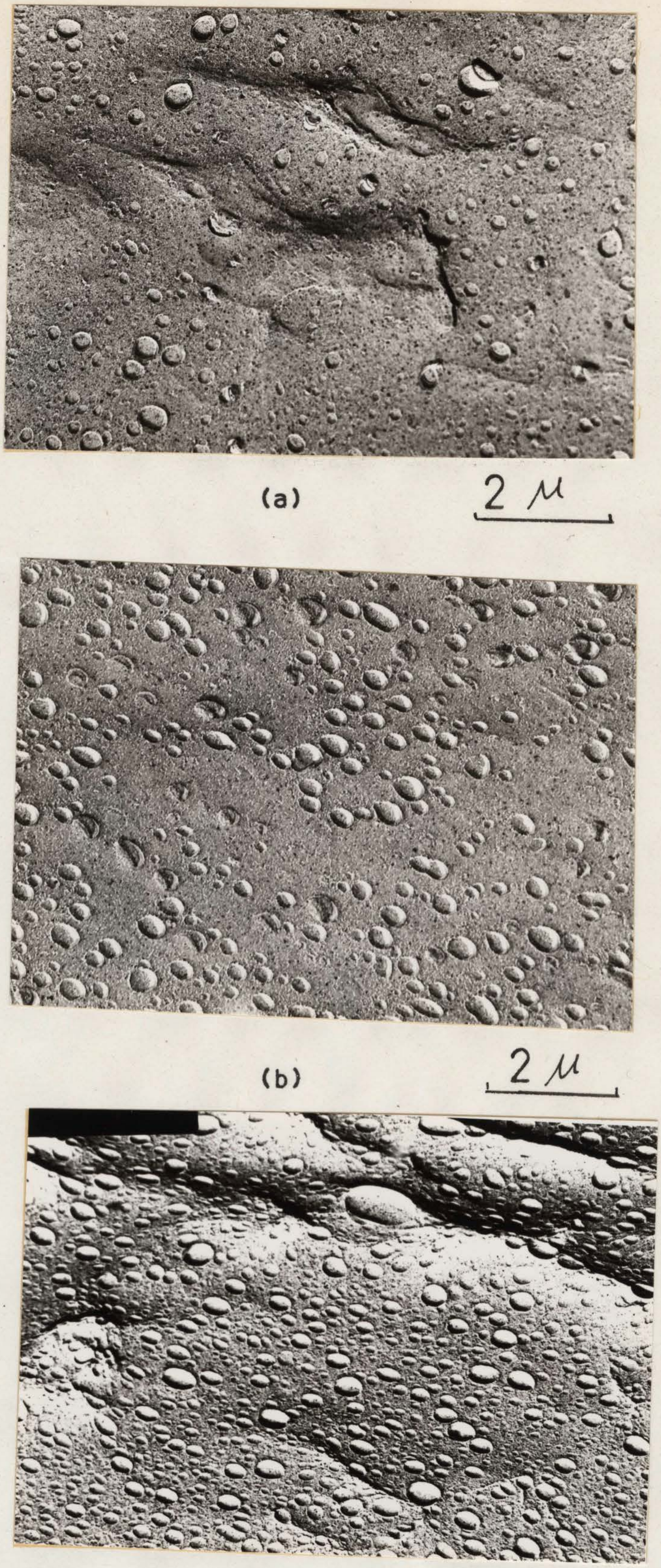

Batch #2

Figure 21. Replicas of PSZ samples thermally shocked from 800°C into a blast of cold air for (a) one cycle, (b) 5 cycles, (c) 10 cycles.

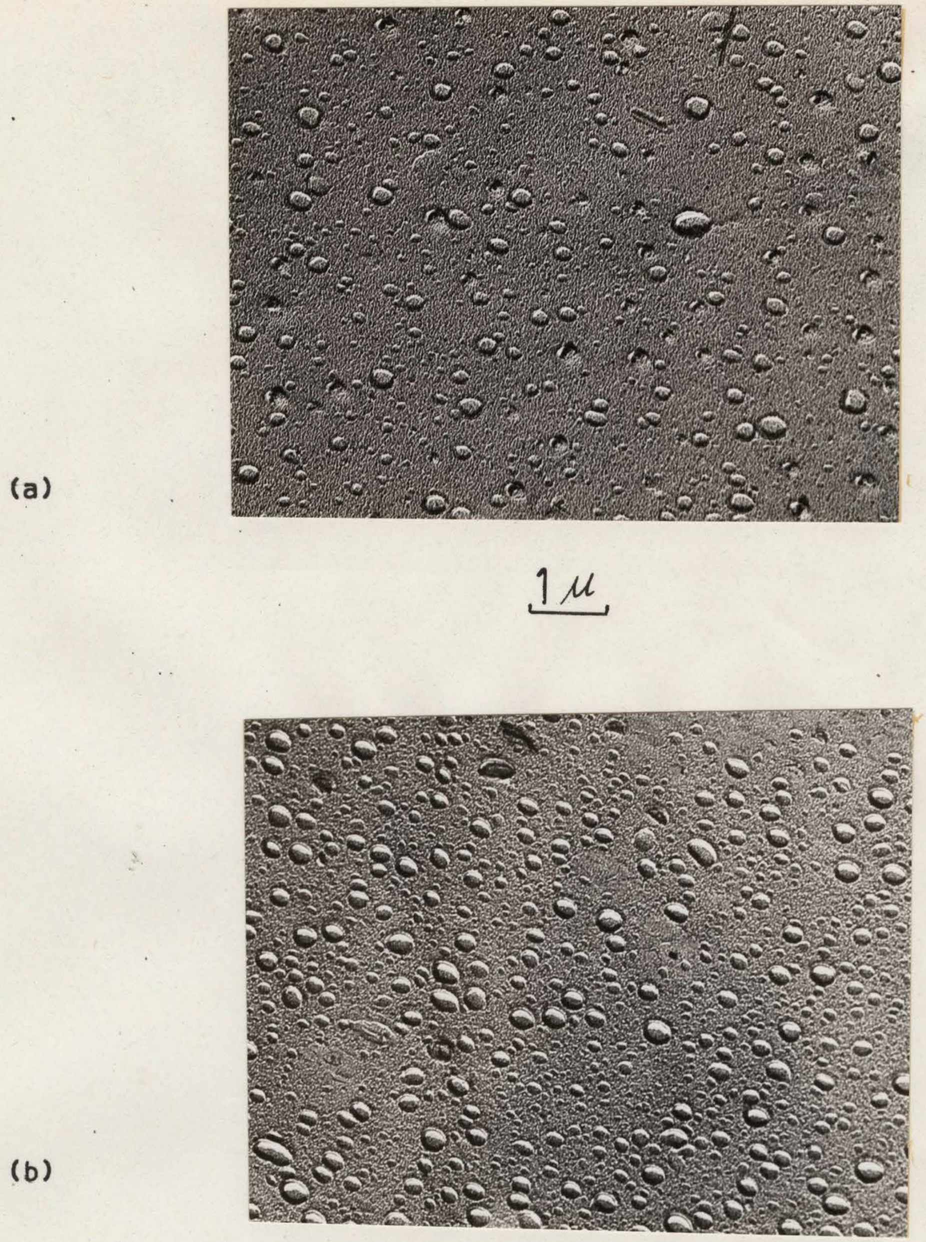

Figure 22. Replicas of PSZ sample thermally shocked from 600°C into water for (a) one cycle and (b) 2 cycles.

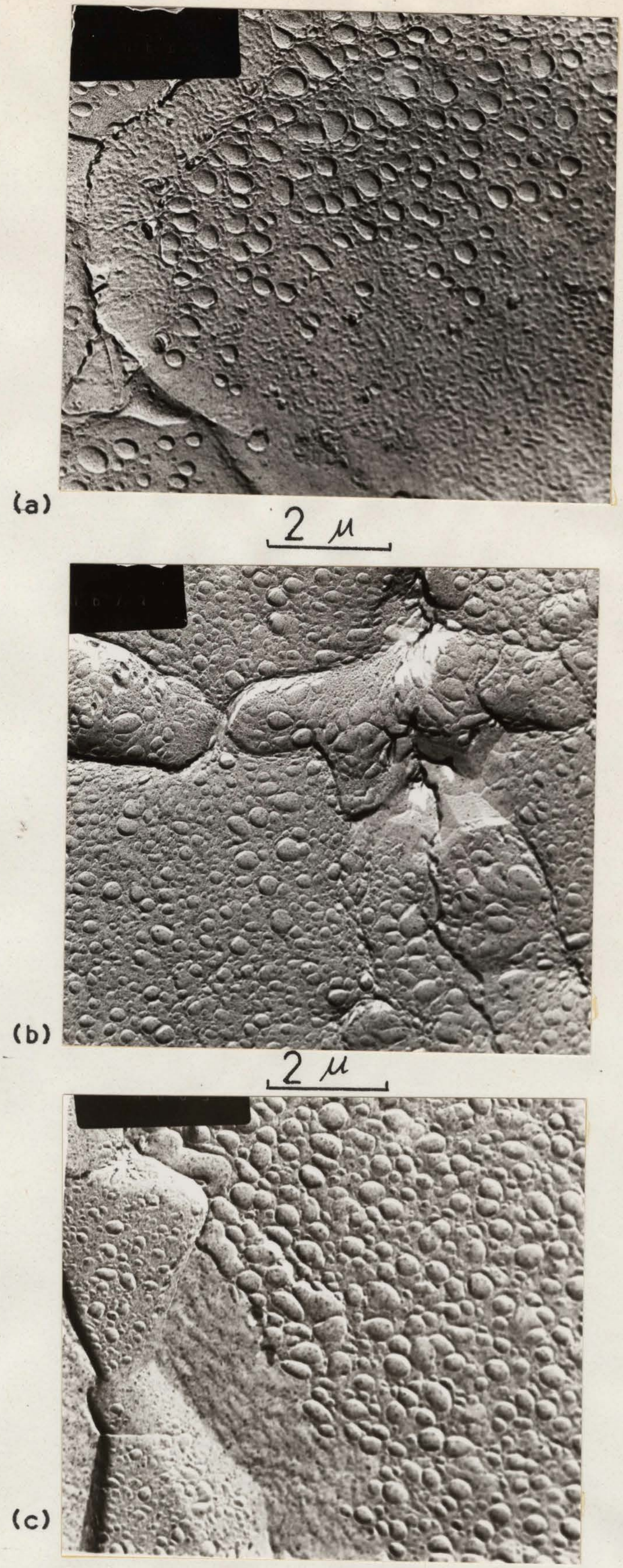

Batch #2

Figure 23. Replicas of PSZ sample thermally shocked from 1100°C into a blast of cold air for (a) one cycle, (b) 5 cycles, (c) 10 cycles.

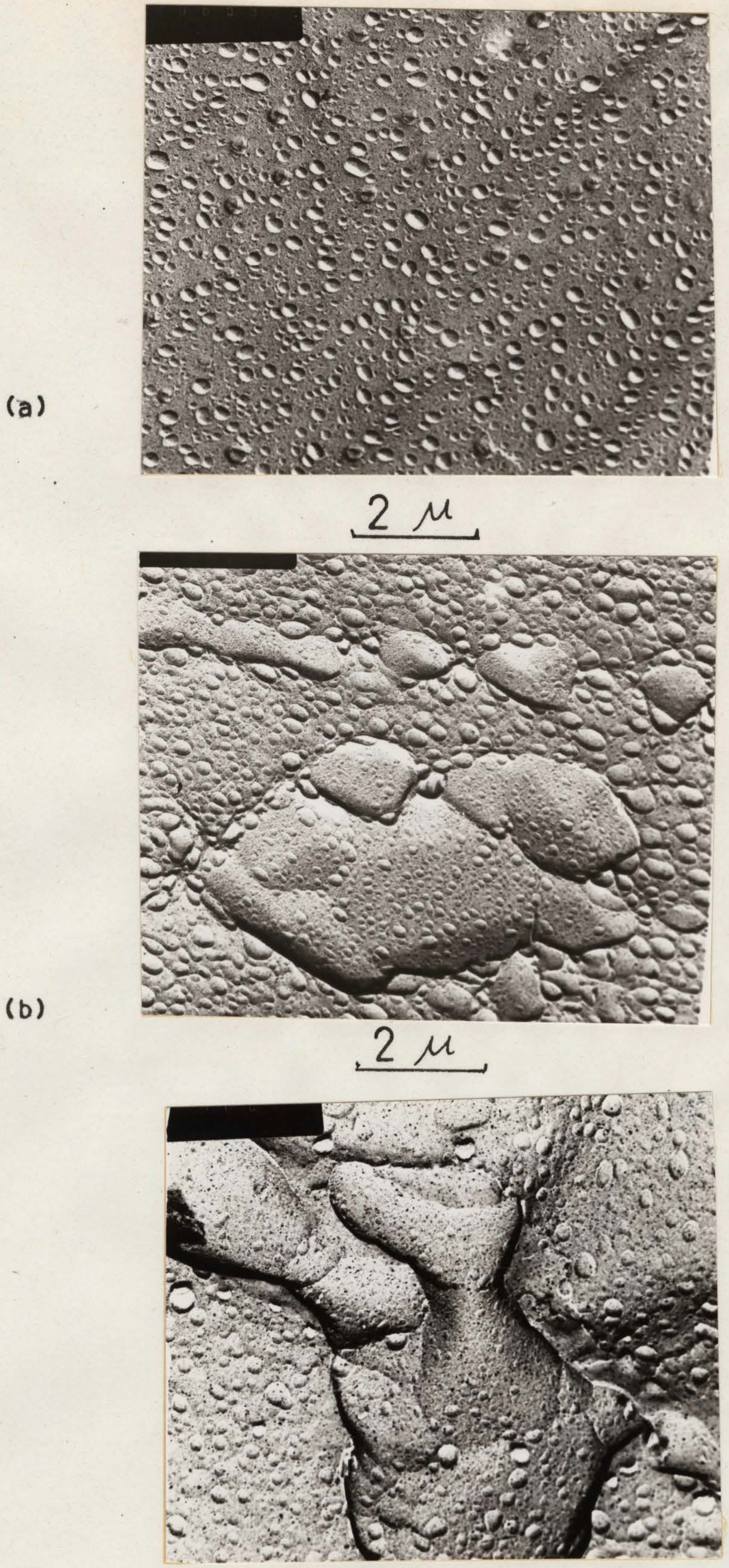

Batch #2

Figure 24. Replicas of PSZ sample thermally shocked from 1200°C into a blast of cold air for (a) one cycle, (b) 5 cycles, (c) 10 cycles.

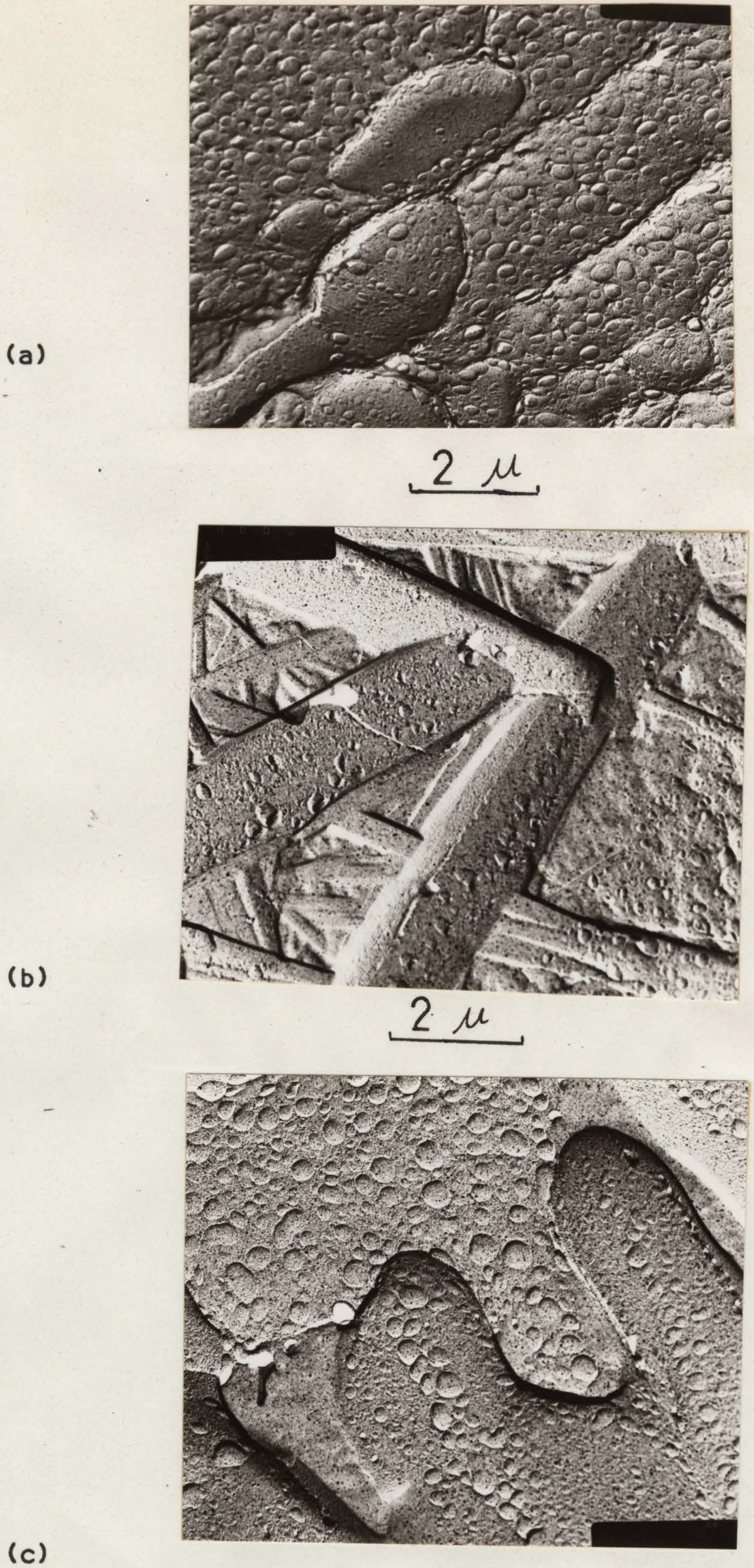

Figure 25. Replicas from PSZ sample thermally shocked from 1300°C into a blast of cold air for (a) one cycle, (b) 3 cycles, and (c) 7 cycles.

Batch #2

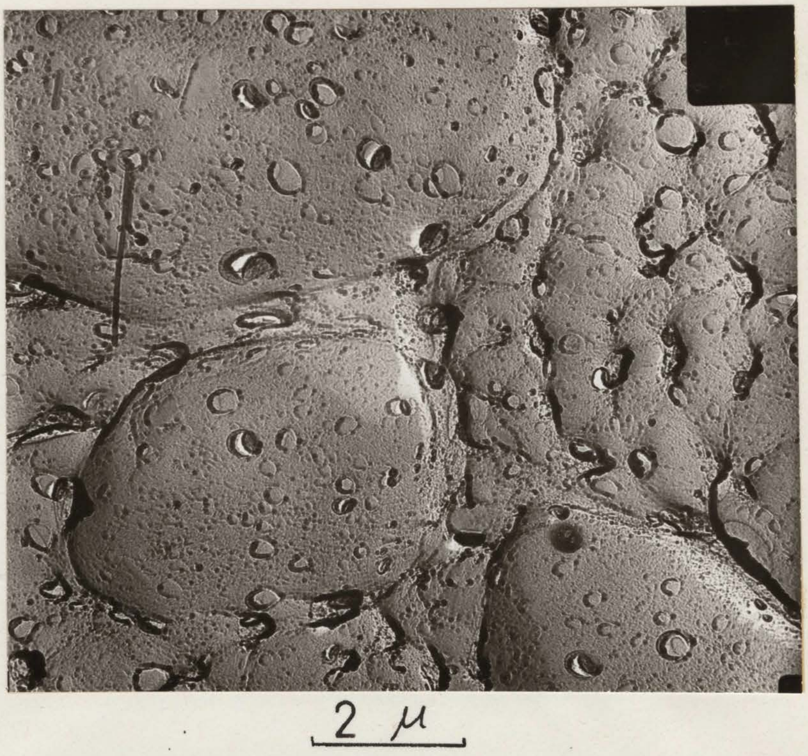

Figure 26. Replicas of PSZ samples thermally shocked from 1100°C into liquid nitrogen for 3 cycles.

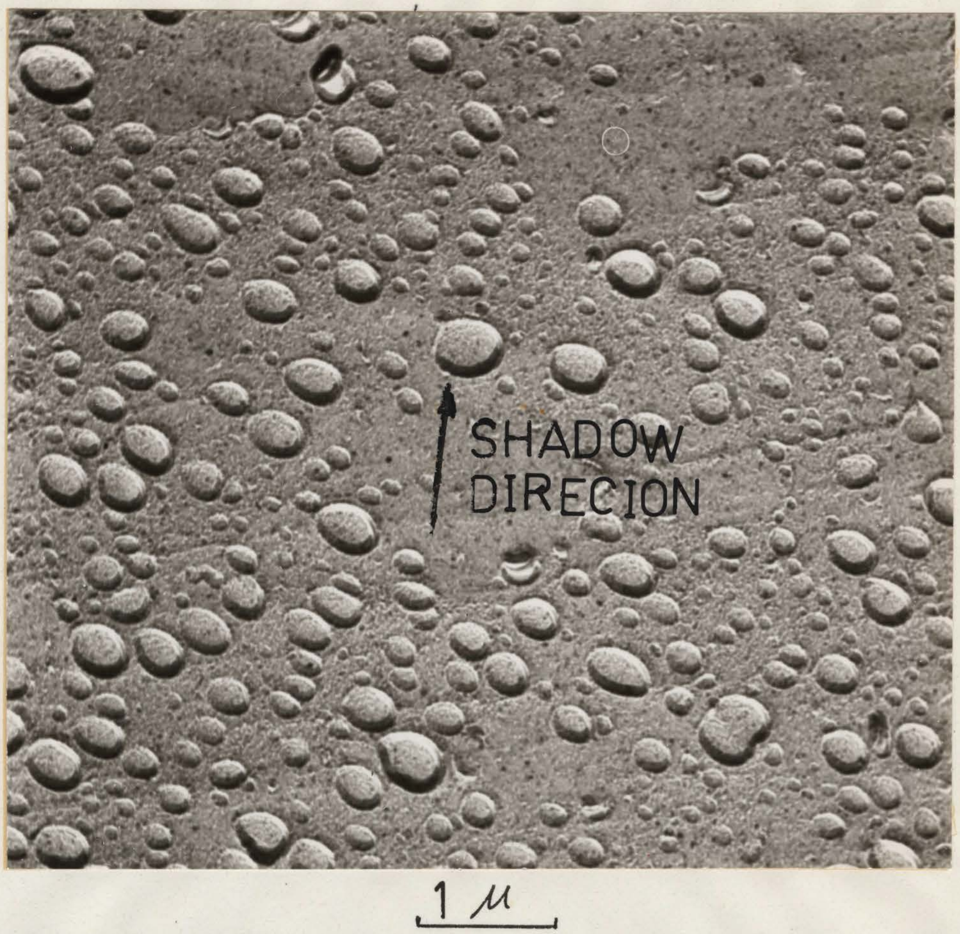

Figure 27. Metal shadowing for PSZ sample thermally shocked from 800°C for 2 cycles into a blast of cold air (batch #2).

In order to investigate whether these large features were in fact depressions or bumps on the surface, replicas were carefully shadowed from a given direction with palladium. As shown in Figure 27, the correlation between the shadow direction and dark sides of the features indicates that these are, in fact, bumps on the surface. Stereo-pairs were also taken of the replicas and when examined with the stereoviewer showed the features to be bumps.

The average size of the bumps as determined by the linear-intercept technique, is ∿ 0.4 μ and this size remains constant for all the different conditions used, including temperature, quenching media and number of shock cycles. It is suggested that this "blistering" phenomenon is possibly due to sub-surface deformation which could throw-up the surface in this fashion. As such, it indicates a degree of plastic flow associated with this material. This follows as the bumps seem coherent with the surface. If the material was totally brittle, the features would constitute "pop-outs" or depressions rather than bumps.

These "bumps" were the main features found on replicas taken from samples thermally shocked from temperatures below normal transformation temperature (< 1100°C). However, replicas taken from samples shocked from temperatures within and above the normal transformation temperature, show the development of facets as well as bumps following thermal shock. Examples of such replicas are shown in Figures 23 to 25. As these are for shock temperatures within and above the normal transformation temperature, the appearance of such features might be expected due to the phase transformation in this material. As this transformation involves $\approx$ 7% volume change, a polished surface should develop roughness accompanying the volume accommodation.

Large platelets with an internal bump structure were observed on replicas taken from samples thermally shocked from 1300°C into a blast of cold air for 3 cycles. Figure 25 shows these platelets. The precursor of this development can be seen following the first shock cycles (Figure 25(a)) in which "folds" appear to develop originating at large surface features. During subsequent cycles, these platelets coalesce, and after 7 cycles the structure takes on a morphology shown in Figure 25(c).

A possible explanation of this sequence is suggested by the following observations:

a) the platelets are large ($\sim$ 15 μ) and of variable size,

b) there does not appear to be any morphological relationship between the platelets themselves, and

c) the platelets develop following a number of thermal shock cycles and no further development but rather a coalescence occurs on subsequent thermal cycling.

Based on considerations (a) and (b) the platelets are not associated with a conventional martensitic-type development as observed in ZrO_2. Martensitic platelets associated with the tetragonal-monoclinic phase transformation in ZrO_2 have been observed to be small(42) (less than 3 μ). Also, the martensite platelets developed bear a definite structural relationship to one another. It can only be assumed, therefore, that the observed development in PSZ is associated with a macroscopic shear process resulting perhaps from the levels of internal stress in the material combined with the thermal shock applied to the material. Effectively, thermal cycling of the material in this fashion could be equivalent in some ways to the "working" of a metal. It is possible that the first few cycles "texture" the pure zirconia component in such a manner as to allow gross platelet development on further application of stress. Such development could reduce subsequent stress concentration levels in the material on further shocking. If this is the case, no further platelet development might be expected on further cycling. Surface energy considerations could then lead to platelet coalescence as observed. It is of interest also to note the disappearance of the "bumps" in some regions adjacent to the platelets. It could be that the process of interfacial motion associated with the appearance of the platelets removes some of these previously produced bumps.

Scanning electron micrographs were also taken from a sample thermally shocked from 1300°C into a blast of cold air for three cycles. The results are shown in Figure 28. Surface roughening and facet development is observed but no platelets are in evidence. The sample examined was from a different bar of PSZ and it could be that insufficient thermal cycles were undertaken to lead to their development.

To determine whether the growth features observed on the 1300°C shock replicas following three cycles were associated with the degree of

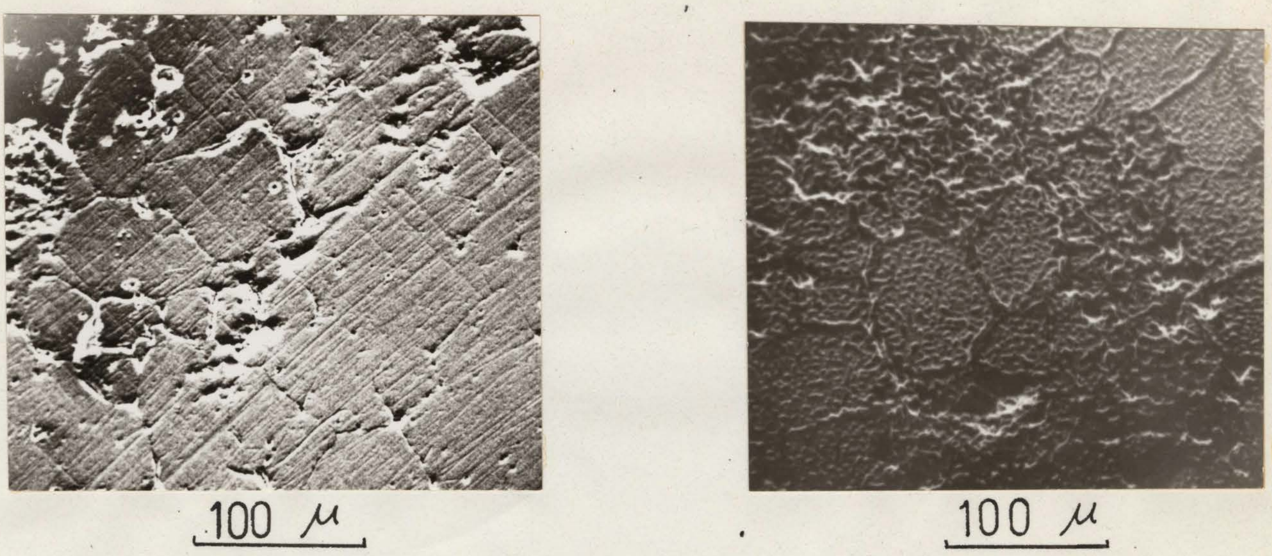

(a) Room temp.

(b)

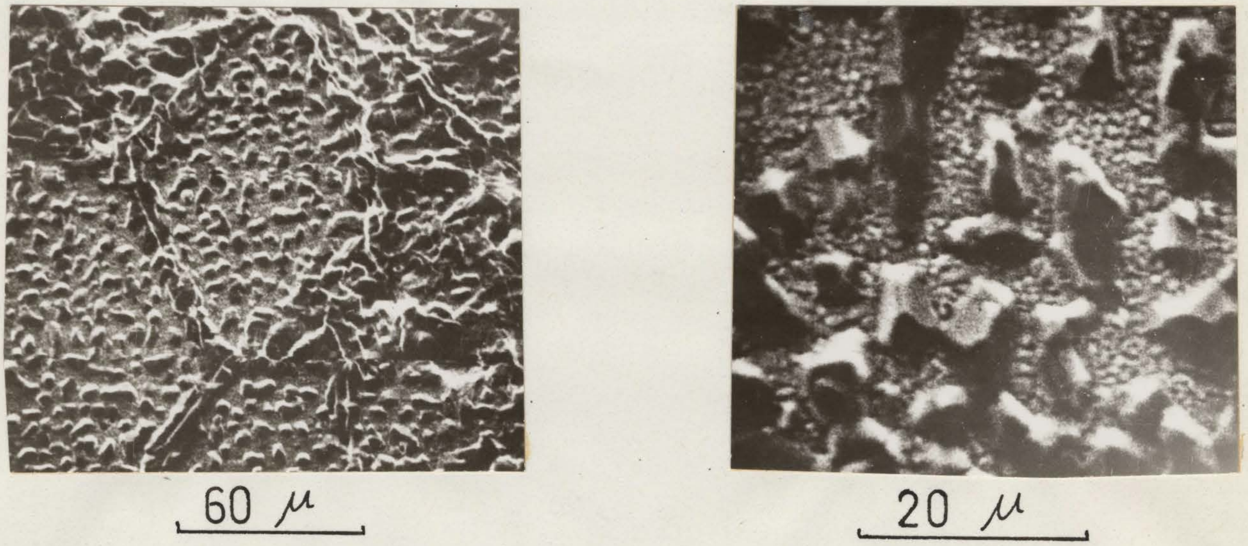

(c)

(d)

Figure 28. Polished PSZ (#2) surfaces following 3 thermal shock cycles from 1300°C (scanning electron micrographs).

shock or the fact that at the 1300°C temperature, the pure zirconia component of the microstructure will all be tetragonal rather than monoclinic or a mixture of the two, samples were shocked from 1100°C for 3 cycles into liquid nitrogen. The degree of shock associated with these tests was considered to be approximately the same as shock from 1300°C into air. Replicas were taken from the surfaces following 3 shock cycles and one is shown in Figure 26. It is evident that there has been no platelet development and only bumps and other surface roughening can be seen. Such platelets did not develop following 10 shock cycles. It would seem, therefore, that the platelet development is associated with the temperature of the shock. At 1300°C, the microstructure contains tetragonal and cubic ZrO_2. On thermal shock, the stress introduced into the system by the transformation will therefore be a maximum. On lowering the temperature to 1100°C the system will contain monoclinic, tetragonal and cubic ZrO_2. Thermal shock from this temperature and consequently, conversion of the tetragonal fraction to monoclinic will stress the system but not to the same level as the 1300°C shock where tetragonal material constitutes 100% of the pure ZrO_2. The degree of shock in both cases is roughly equivalent so the strain associated with the cubic ZrO_2 will be the same and so also will be the associated stress. The development of platelets therefore must be associated with the pure ZrO_2 component. It would appear that it must be 100% tetragonal, however, as will be seen later, holding PSZ samples at 1300°C for a week does not induce platelet transformation. Consequently, the fraction tetragonal does not appear to control the process. The thermal shock component of the cycle is evidently most important. These facts all indicate the role of stress in the development of the observed morphology and supports the proposed explanation.

Fine twins, ≈ 1000 Å in size, were observed on the replicas taken after thermal shocking from above and below the normal transformation temperature region when examined at high magnifications. Some of the electron micrographs obtained for samples thermally shocked from different temperatures into water and cold air for different numbers of cycles are shown in Figures 29 - 31. Figures 29 and 30 show replicas from samples thermally shocked from 600° and 700°C into water and cold air respectively. It seems that thermal stresses induced during the first shock cycle are sufficient to nucleate twins which appear more clearly on subsequent cycles. Replicas taken from a sample thermally shocked from 1300°C into a blast of cold air for one and ten cycles are shown in Figure 31. Because 1300°C is above the normal transformation temperature, the appearance of such twins at this temperature might be expected due to the phase transformation in this material on shocking from such a temperature.

The production of twins on the transformation of pure zirconia from the tetragonal modification to the monoclinic modification is well documented. Bailey(55) reported that the transformation in a pure zirconia is a shear-type martensitic process and the monoclinic phase formed on cooling through the transition temperature is generally twinned. Fine twinning of the order of 1000 Å is generally observed in martensite in the metallurgical systems most extensively studied(57,58). Fine scale twinning has also been observed on the transformation of thin films(59), although it is known that the transformation characteristics of thin

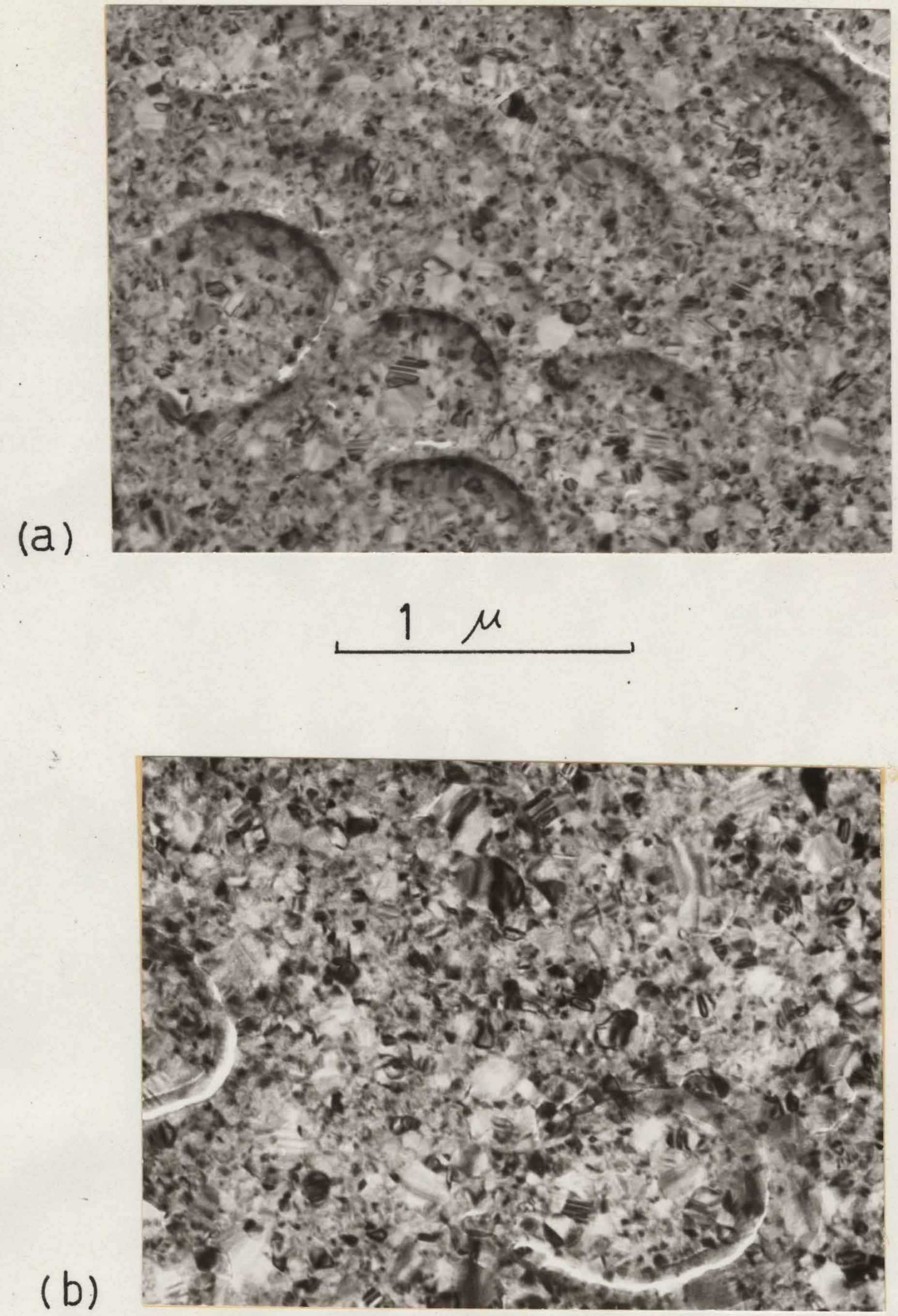

Figure 29. Replicas of PSZ samples thermally shocked from 600°C into water for (a) one cycle, and (b) four cycles.

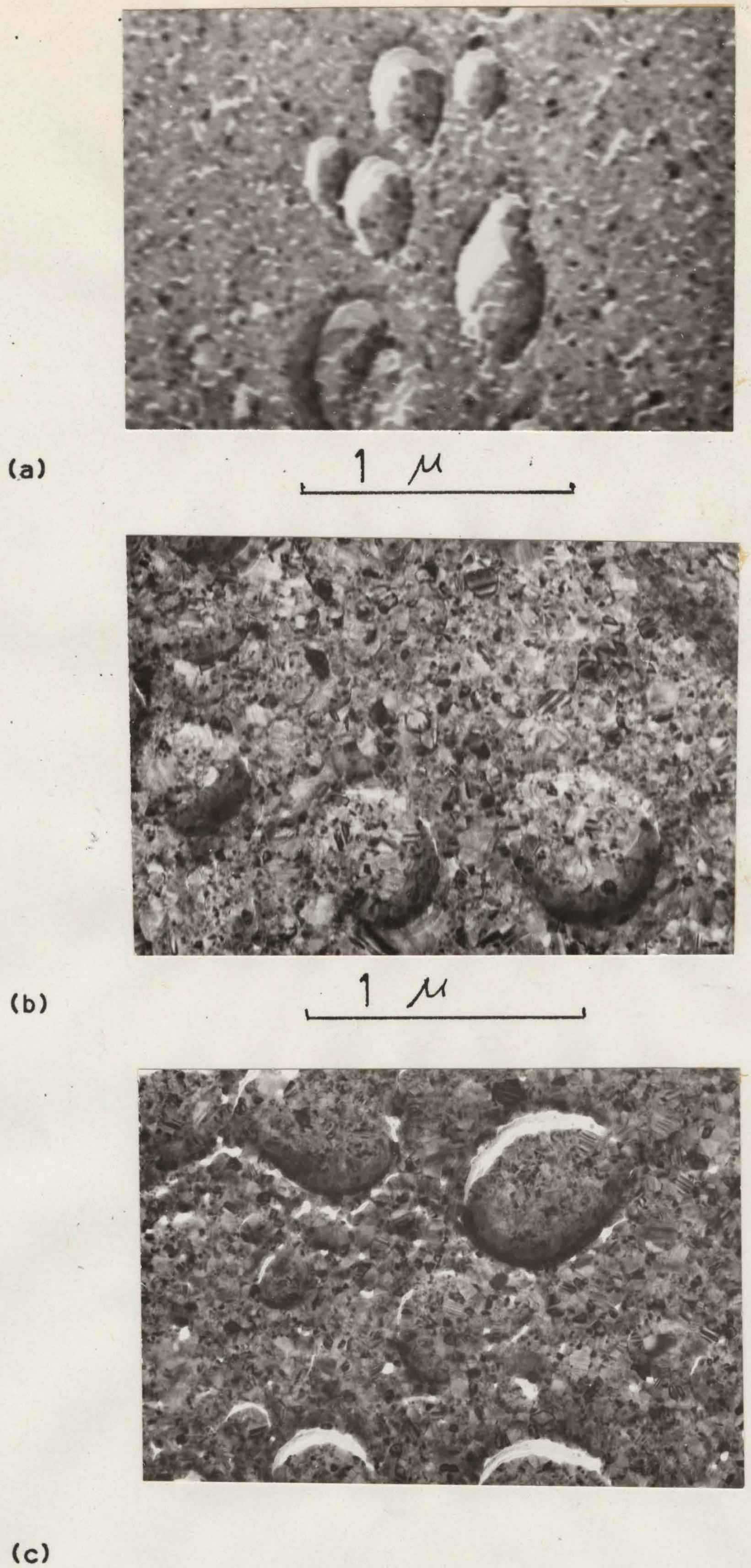

Figure 30. Replicas of PSZ sample thermally shocked from 700°C into a blast of cold air for (a) one cycle, (b) five cycles, (c) 10 cycles.

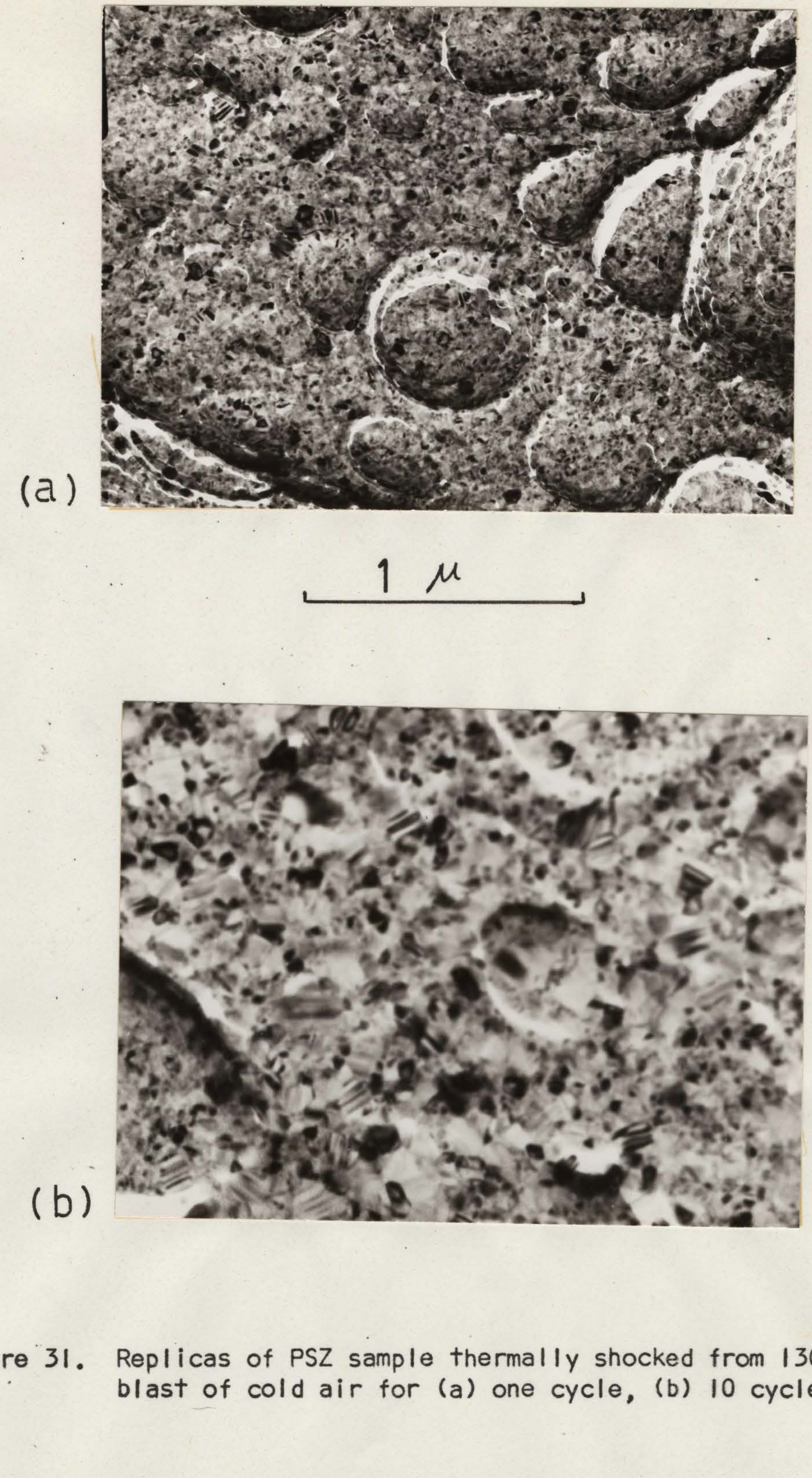

Figure 31. Replicas of PSZ sample thermally shocked from 1300°C into a blast of cold air for (a) one cycle, (b) 10 cycles.

films differ somewhat from the bulk material.

Electron diffraction techniques indicated that the twinned material is actually on the replica, suggesting that the twinning process separates the twinning material from the matrix and the loosened material is then "lifted" from the surface by the replica. The electron diffraction patterns also show that some cubic material is extracted from the sample in the same fashion. A typical pattern of a replica is shown in Figure 32. No such pattern would be expected from a clean replica.

The appearance of twins on the replicas taken from the surfaces of polished thermally shocked samples raises a question as to whether these twins in fact existed on the original unshocked polished surfaces and the thermal shock merely loosens them and allows the replica to pick them up. To investigate this possibility, the polished surface of a PSZ sample was scratched with a diamond stylus attached to a microhardness tester. Replicas were then taken around the position of the scratch and examined in the electron microscope. One such replica is shown in Figure 33. The line of the scratch is clearly evident across this figure. An electron diffraction pattern taken from the same replica is shown in the same figure and indicates that surface debris was extracted by the replica in this case. The non-appearance of any twins indicates that their observation on replicas taken following thermal shock must be associated with the shock process. It is interesting to note that the twins appear inside the "bumps". This suggests that the bumps are not intrinsic microstructural features per se and supports the hypothesis of their association with sub-surface deformation.

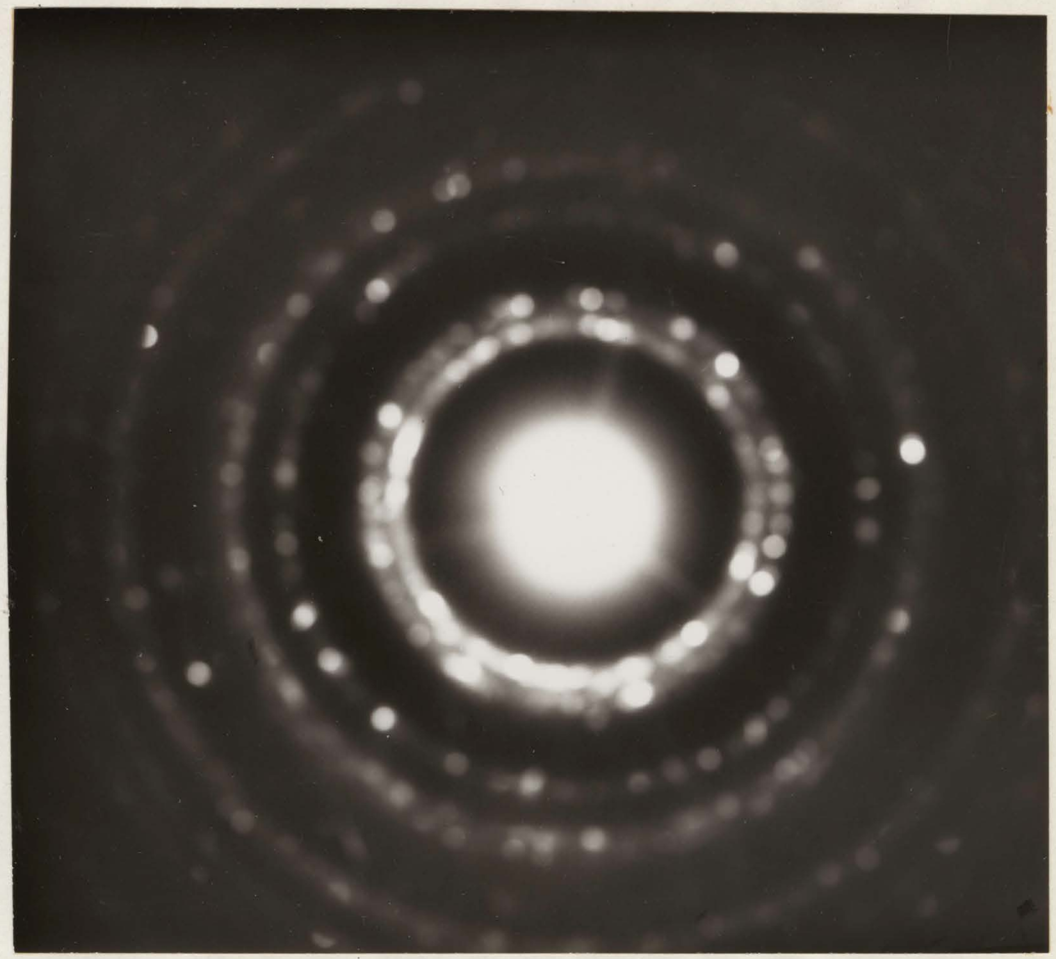

Figure 32. A diffraction pattern taken from a replica of PSZ sample thermally shocked from 1100°C for 4 cycles into a blast of cold air.

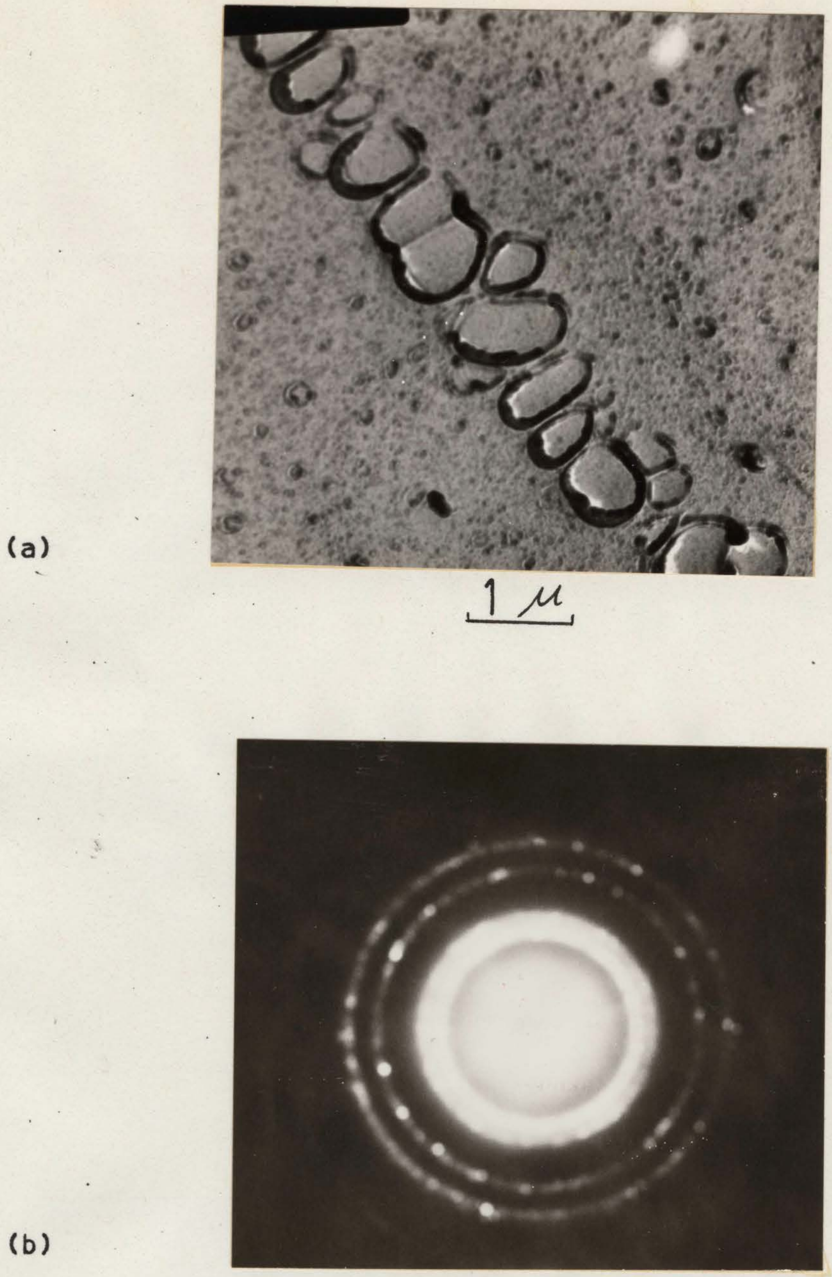

Figure 33 (a) Replica of a scratched sample of PSZ at room temperature.
(b) Diffraction pattern taken from the scratched sample.

The nature of the twin production process was investigated by thermally shocking two halves of a polished PSZ bar from the same furnace. Both halves were thermally shocked from 900°C into cold water three times from the same furnace and replicas taken from each. Following this one half was shocked a further 7 times whilst the other half was allowed to anneal (in the furnace) for the time involved. Replicas were taken from the same location on each bar following the conclusion of the test. The replicas involved are shown in Figures 34 and 35. From these micrographs it can be seen that no further twin development occurred during the anneal following the three thermal shocks whereas significant development accompanied the extra seven cycles experienced by the other half of the bar. This would seem to indicate that these twins are stress induced. Further evidence on this point was obtained on thermal shocking two halves of a bar of batch #2 material from 600°C, one into air and the other into cold water. The air quench produced no detectable twins on the replicas whereas the water quench (Figure 29(a)) produced a significant number. A water quench is much more severe and therefore induces higher stresses than an air quench.

As twinning is known to accompany the transformation of tetragonal to monoclinic ZrO_2, the observation of such twins at sub-transformation temperatures suggests that the transformation has occurred at such temperatures.

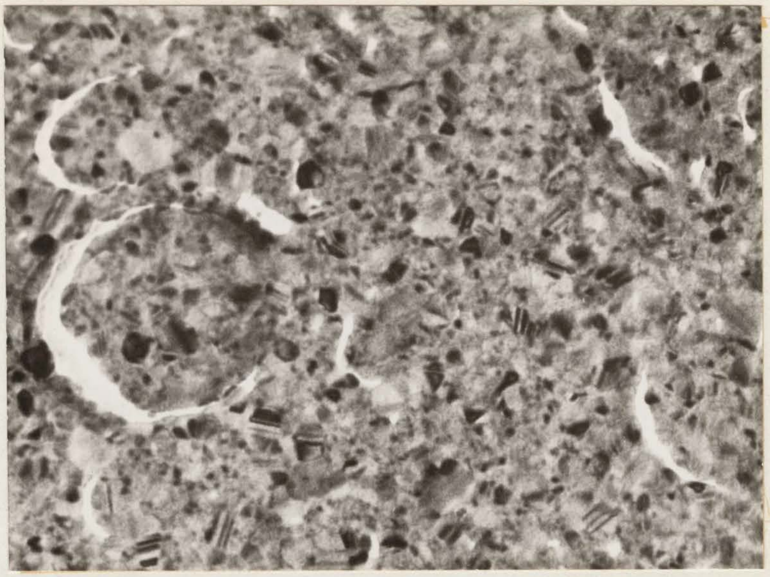

(a)

Replica following 3 thermal shocks.

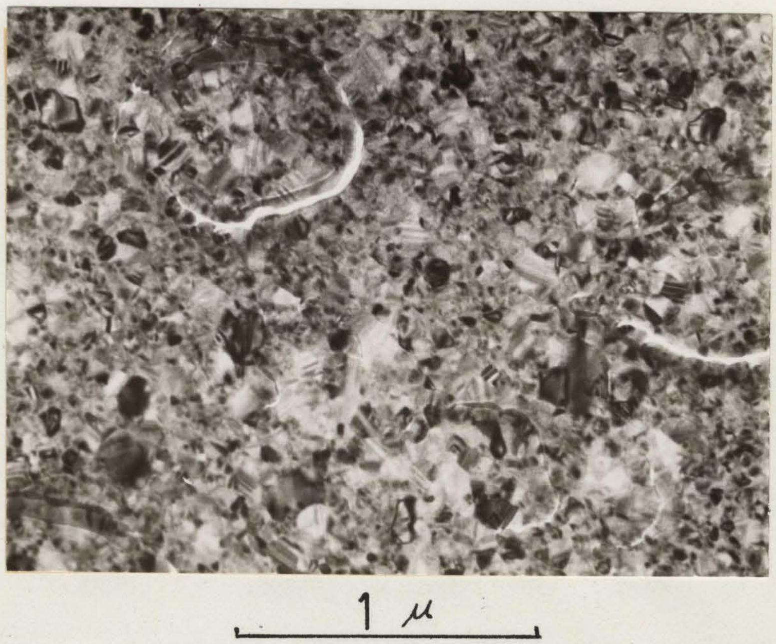

(b)

Replica following subsequent anneal and slow cooling.

Figure 34

(a)

1 μ

Replica following 3 thermal shocks.

(b)

Replica following 10 thermal shocks.

1 μ

Figure 35

4.2.2 Batch # 1

Replicas taken from PSZ samples of batch #1, thermally shocked from different temperatures into a blast of cold air are shown in Figures 36 and 37. There is some evidence of surface features developing even at low temperatures and on increasing the shock temperature these features become more pronounced. From 1100°C of shock on up, second-phase particles seem to separate from the rest of the specimen and cracks seem to appear associated with these particles. This is particularly noticeable in the 1200°C specimen as shown in Figure 37(b). These observations are significantly different from those observed in batch #2. It has been demonstrated by dilatometric measurements(70) that the level of internal stress in batch #1 (40,000 psi maximum) is significantly higher than at batch #2 (20,000 psi maximum) following fabrication. This is understandable based on the rapid quench of batch #2 and the consequent relief of much of the internal stress by grain boundary decohesion. Much evidence is available to support this explanation(70). This being the case, microcracks might be expected to develop on the thermal shocking of batch #1 as observed on the replicas. Another possible explanation could be the larger amount of cubic phase in batch #2 (Table III). This will not only reduce the volume fraction of transforming material but would increase the "plasticity" of the PSZ body. Some evidence is available that the cubic component of PSZ bodies can act in a ductile fashion and that it is hardened by increasing its lime content(5). As shown in Table III, the lime level in both batches is the same and it can only reside in the cubic

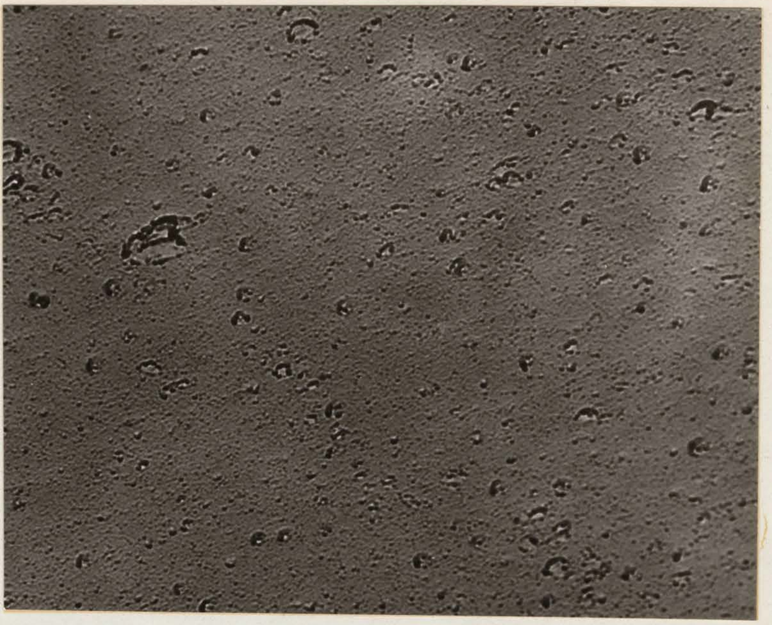

1 μ

(a) Replica of PSZ sample at room temperature.

(b) Replica of PSZ thermally shocked from 800°C into a blast of cold air for one cycle (batch #1).

Figure 36

(a) Replica of PSZ sample shocked from 1100°C into a blast of cold air for one cycle.

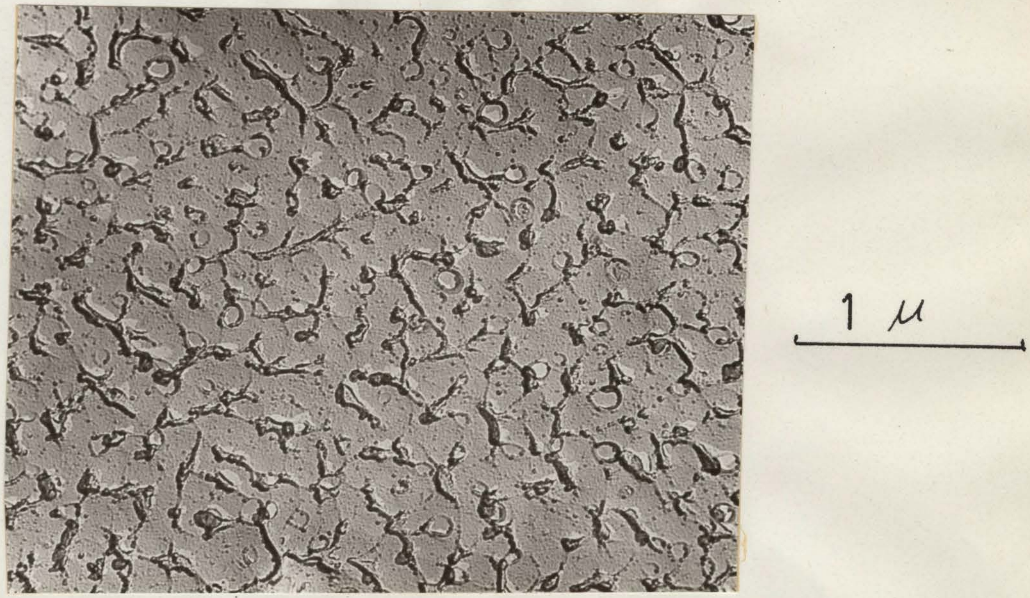

(b) Replica of PSZ sample shocked from 1200°C into a blast of cold air for one cycle.

Figure 37

TABLE III

Batch #	Wt.% CaO	Wt.% Monoclinic
1	3.4	40
2	3.4	27

phase, this phase in batch #2 will be softer than that in batch #1. These factors could also lead to the non-appearance of microcracking on the batch #2 replicas. It is also interesting to note the non-appearance of bumps and twins on the batch #1 replicas. The nonappearance of coherent bumps and the observation of cracking is further evidence in favour of the brittle nature of the batch #1 material. Monoclinic ZrO_2 is noted to twin most readily when totally confined(55). The cracking observed in batch #1 possibly relaxes the confinement of the monoclinic material and twinning does not therefore occur. Essentially, it is being suggested that batch #1 is a more "brittle" system than batch #2.

By the linear-intercept technique the number of cracks per unit area of sample was determined from the replica (Figure 37(b)). Assuming that such cracks were uniformly distributed throughout the material volume, the crack density was determined as $\sim 10^7$ cracks/cc. It is of interest to discuss this phenomenon in terms of Hasselman's analysis(79) of thermal shock resistance. As outlined, Hasselman demonstrated that the critical temperature difference required for crack instability is given by:

$$\Delta T_c = [2G/\pi \ell \alpha^2 E]^{1/2} \; (1 + 2\pi N \ell^2)$$

where N is the crack density (cracks/unit area), ℓ is the crack half-length, E is Young's modulus, α is the thermal expansion coefficient and G is the shear modulus.

It can be shown that the crack length (ℓ_{min}) which separates the kinetic crack propagation region from that of quasi-static propagation is proportional to N in the following manner:

$$\ell_{min} \propto \sqrt{1/N}$$

Therefore, a large value of N will shift the minimum to very small crack lengths. Particularly then, it is suggested that due to the large number of cracks in batch #1 PSZ, quasi-static crack propagation is exclusively observed and the body maintains a large portion of its strength even after continuous thermal cycling. As reported by Hasselman, the introduction of a crack into a stressed body is equivalent to lowering the Young's modulus of the body. The total energy in a thermally shocked body is the sum of the elastic stored energy and the surface energy associated with produced cracks. The greater the number of microcracks produced, the higher the second energy term. Hence, for a given total energy, the elastic stored energy is reduced by microcracking.

4.2.3 General Discussion

It is evident that all replicas taken from PSZ samples following thermal shock show surface roughening. Such roughening could be associated with at least three phenomena, i.e.,:

(i) a non-equilibrium microstructure following fabrication,

(ii) thermal etching, and
(iii) the phase transformation of the pure zirconia component of the microstructure.

In view of the possible non-equilibrium state of the PSZ microstructure, it is possible that the features observed represent microstructural adjustments during the high temperature soak period associated with each thermal shock cycle. The highest temperature used in the thermal shock tests was 1300°C. To investigate this possibility, polished samples were placed in furnaces at 900 and 1300°C and held at these temperatures for one week, and then slowly cooled to room temperature. Replicas were then taken from both and compared with the initial ones. The replicas obtained from the 1300°C tests on batch #2 are shown in Figure 38. It can be seen that no significant changes in the replica structures have occurred during the anneal. The same observations were made for batch #1. Consequently, it would appear that non-equilibrium conditions do not account for the roughening. The same was observed in the case of the 900°C replicas.

Thermal etching is unlikely at temperatures $< 1000^{\circ}$C and, in fact, replicas taken from slowly-cooled polished bars appeared the same as the original ones. Therefore, thermal etching is not responsible for the observed roughening.

It is therefore reasonable to expect that the roughening observed on all the replicas is associated with the phase transformation of pure zirconia component of the PSZ material. As mentioned in the literature

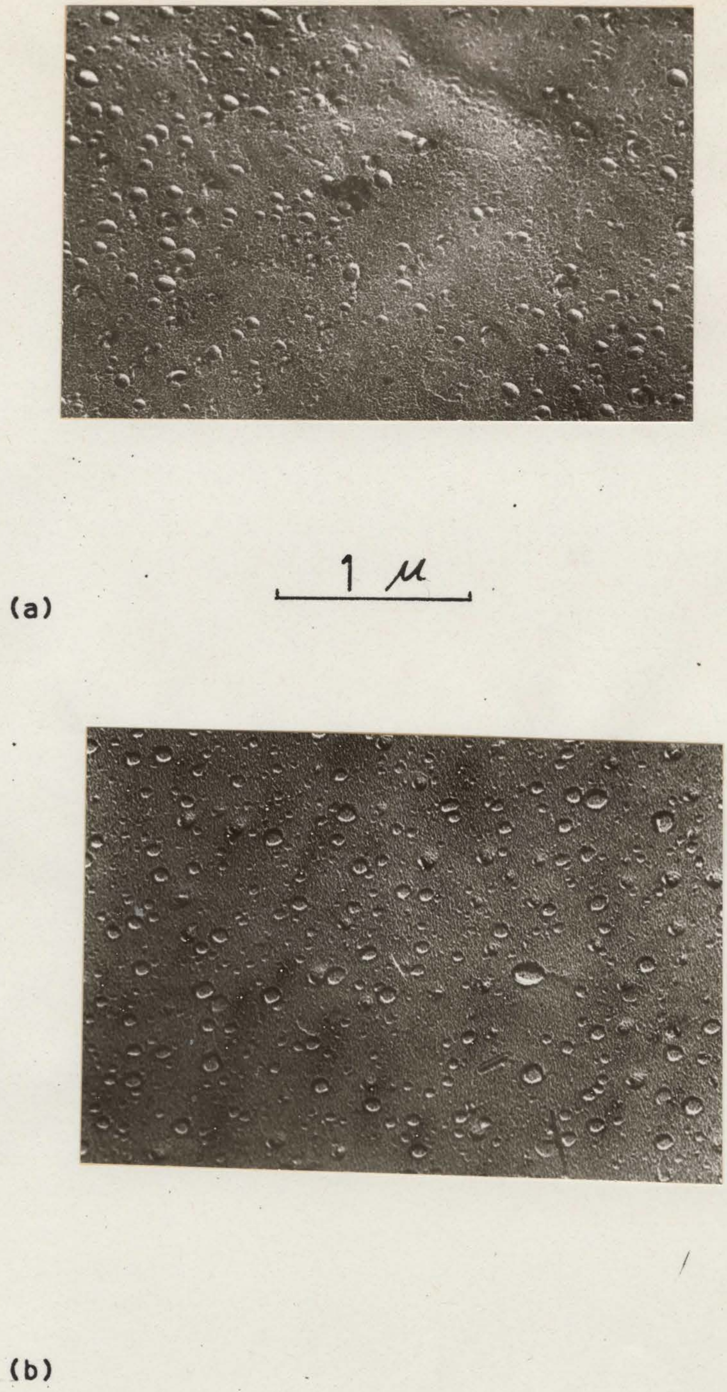

Figure 38. Replicas of polished PSZ surface before (a) and after (b) annealing at 1300°C for one week.

review, the reversible transformation of pure zirconia has been studied by many workers. The transformation is accompanied by volume expansion (∿ 7%) on cooling. As reported recently by Bansal and Heuer(62), surface relief accompanied the transformation in both directions.

It is easy to understand that the surface roughening observed on replicas for temperatures within and above the normal transformation temperature might result from the tetragonal $\rightleftarrows$ monoclinic transformation in the material. It is suggested, therefore, that the roughening observed below the normal transformation temperature region is possibly due to the transformation also and its induction by stresses on the material. In other words, the presence of internal stresses together with thermal shock induced stresses may cause the transformation to occur at sub-transformation temperatures.

Garvie and Nicholson(4) offered a model for thermal shock resistance of batch #I type CaO-PSZ, based on stress induction of the phase transformation. Close examination of the replica shown in Figure 37(b) suggests that grains and cracks are associated. They point out that the most probable source of crack initiation in batch #I PSZ is the monoclinic-tetragonal transformation in the pure ZrO_2 component. This mechanism is easily understood for shock temperatures above and during the phase transformation. The expansion of the tetragonal component on transforming to monoclinic in a contracting body will produce cracks. They suggested that the same mechanism produces cracks below normal transformation temperatures owing to thermal stress induction of the transformation.

The proposed model is shown schematically in Figure 39. At sub-transformation temepratures the stress acting on a monoclinic domain in thermal shock probably consists of two components, the internal stress residual following fabrication (σ_i) and the thermal shock stress (σ_{th}), i.e.,

$$\sigma_{total} = \sigma_i + \sigma_{th}$$

A critical value of σ_{total} is required to trip the transformation of the domain at a given sub-transition temperature. For a given σ_i, therefore, more domains will be tripped, the greater the ΔT_{shock}. The transformation is associated with $\stackrel{\sim}{\sim}$ 7% contraction on heating and consequent interfacial separation of the domains and the matrix. The tensile stresses in the matrix are thus relieved and the matrix contracts somewhat into the space left around the now-tetragonal domain. An overall lowering of the stress level in the body results and the tetragonal-monoclinic reversion will then occur at sub-transition temperatures. The accompanying volume increase punches cracks into the matrix around each monoclinic domain. Now batch #2 material also exhibits superior thermal shock resistance, and therefore a stress relieving mechanism must also be operating. The non-observation of cracks negates the application of Hasselman's analysis in this case. However, an equivalent model to explain the behaviour of batch #2 material could follow steps I to 3 of the Garvie-Nicholson model but instead of producing cracks in passing from step 3 to step 4, the cubic matrix could plastically deform and the consequent back-stresses cause the monoclinic domains to twin.

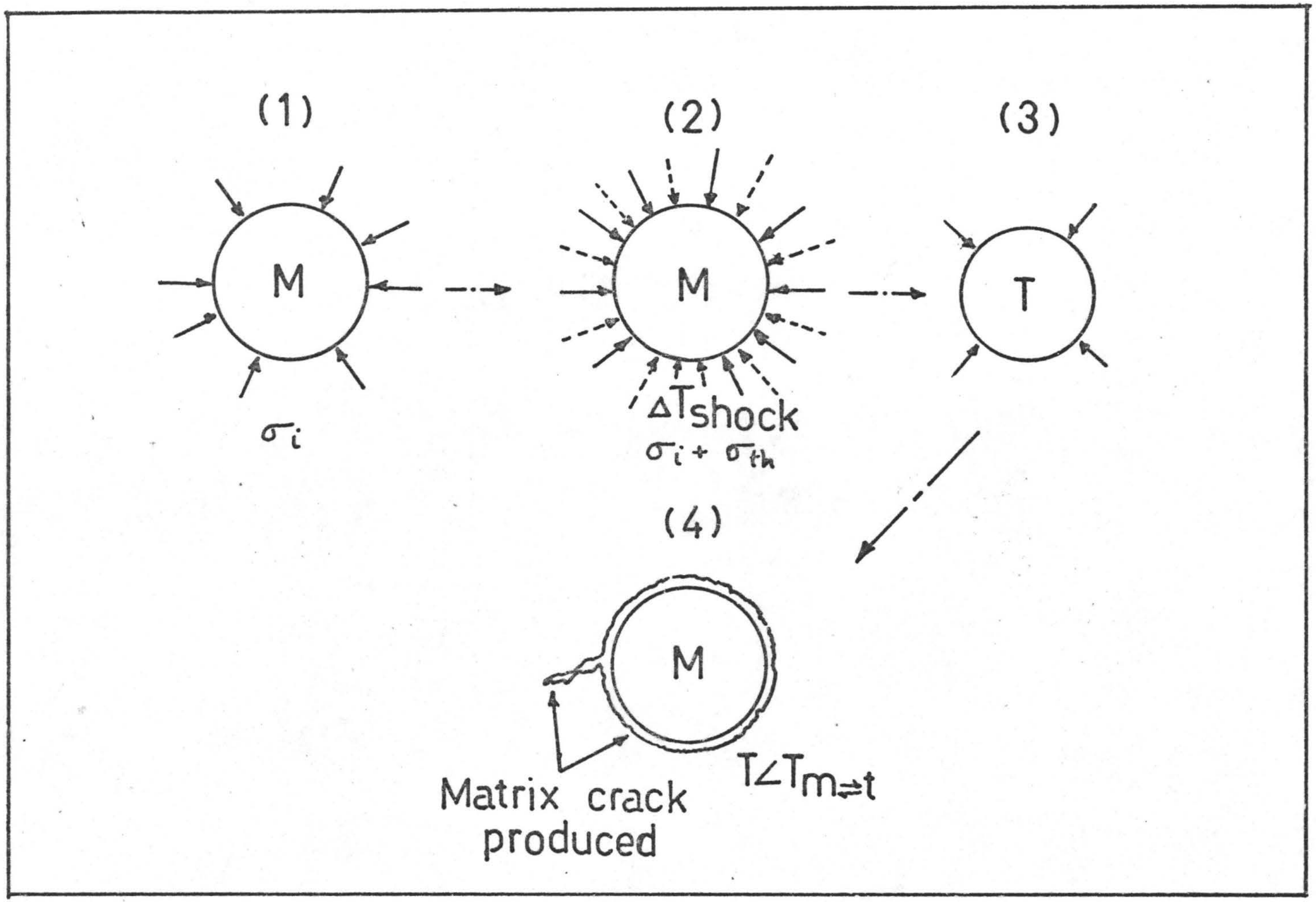

STRESS MODEL

Figure 39

Further evidence in favour of both these models will now be presented. Evidence for the triggering of the monoclinic-tetragonal transformation at sub-transformation temperatures in batch #1 was obtained by studying the phenomenon of ratchetting(4). Data obtained at sub-transformation temperatures (see Figure 14) indicates that a steady state ratchetting condition is realised above 2 or 3 cycles and no further elongation occurs. That ratchetting takes place at sub-transition temperatures is evidence for the occurrence of the phase transformation at these temperatures, as only cracking can give rise to such an expansion.

If the volume expansion associated with the tetragonal-monoclinic transformation causes development of microcracking within the material and the observed ratchetting, then the density of the bulk material should change. Density measurements were made on thermally shocked samples of batch #1, and plots of the reciprocal density versus the number of thermal shock cycles at different temperatures are shown in Figures 40 - 42. It can be seen that the reciprocal-density data agree well with the ratchetting data (Figure 14).

Batch #2 material, on the other hand, showed an increase in density to a constant value on thermal shock from 900°C (Figure 43). This could result from the filling up of residual fabrication porosity by stress-induced sintering accompanying the t → m phase transformation. The high level of cubic phase in this material and its possible ductility could lead to an internal "hot-pressing" process in which the compression is supplied by the t → m transformation. Chaklader et al.(86) have demonstrated that pure ZrO_2 can be hot pressed to theoretical density at these

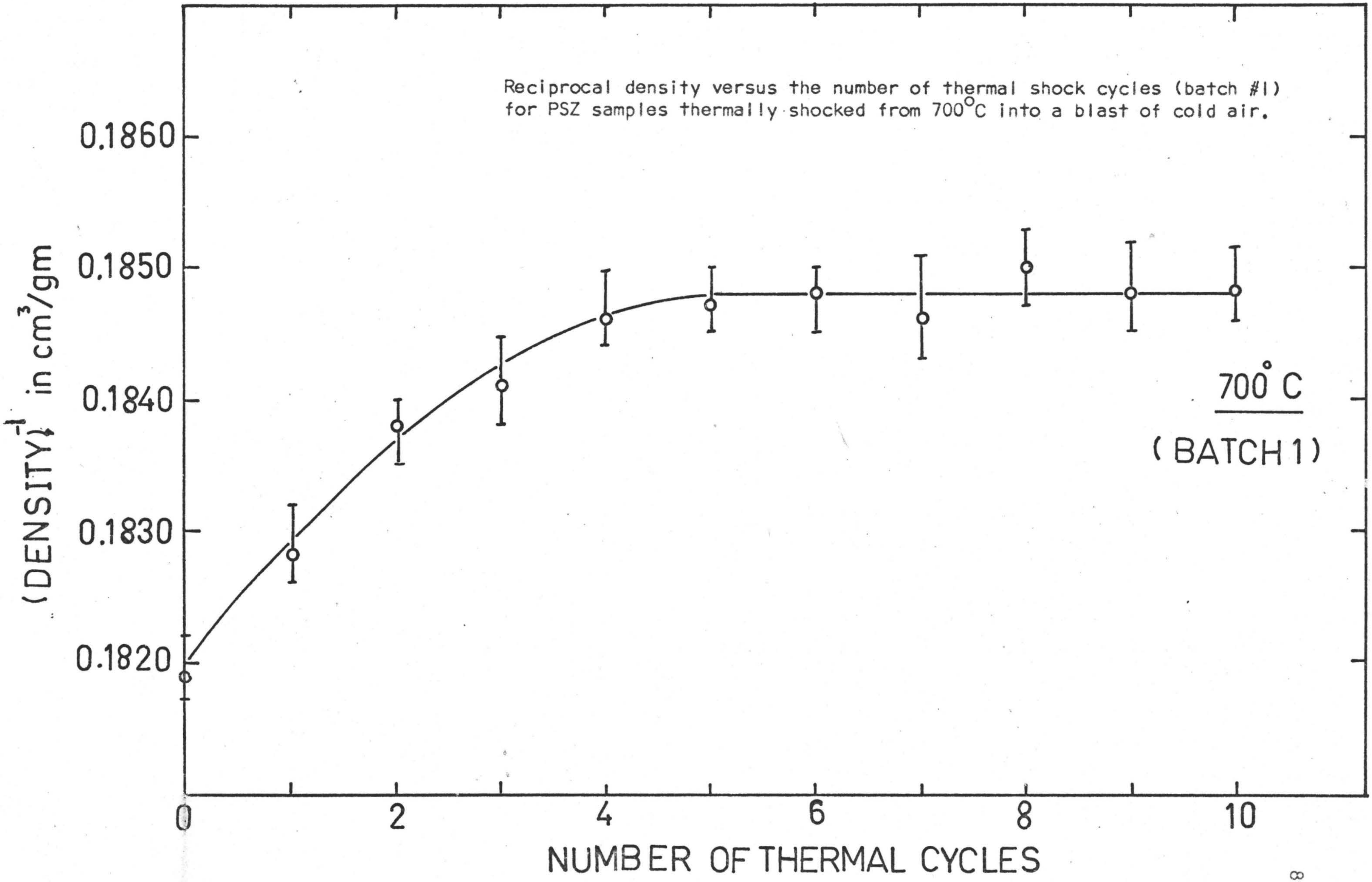

Reciprocal density versus the number of thermal shock cycles (batch #1) for PSZ samples thermally shocked from 700°C into a blast of cold air.

FIG. 40

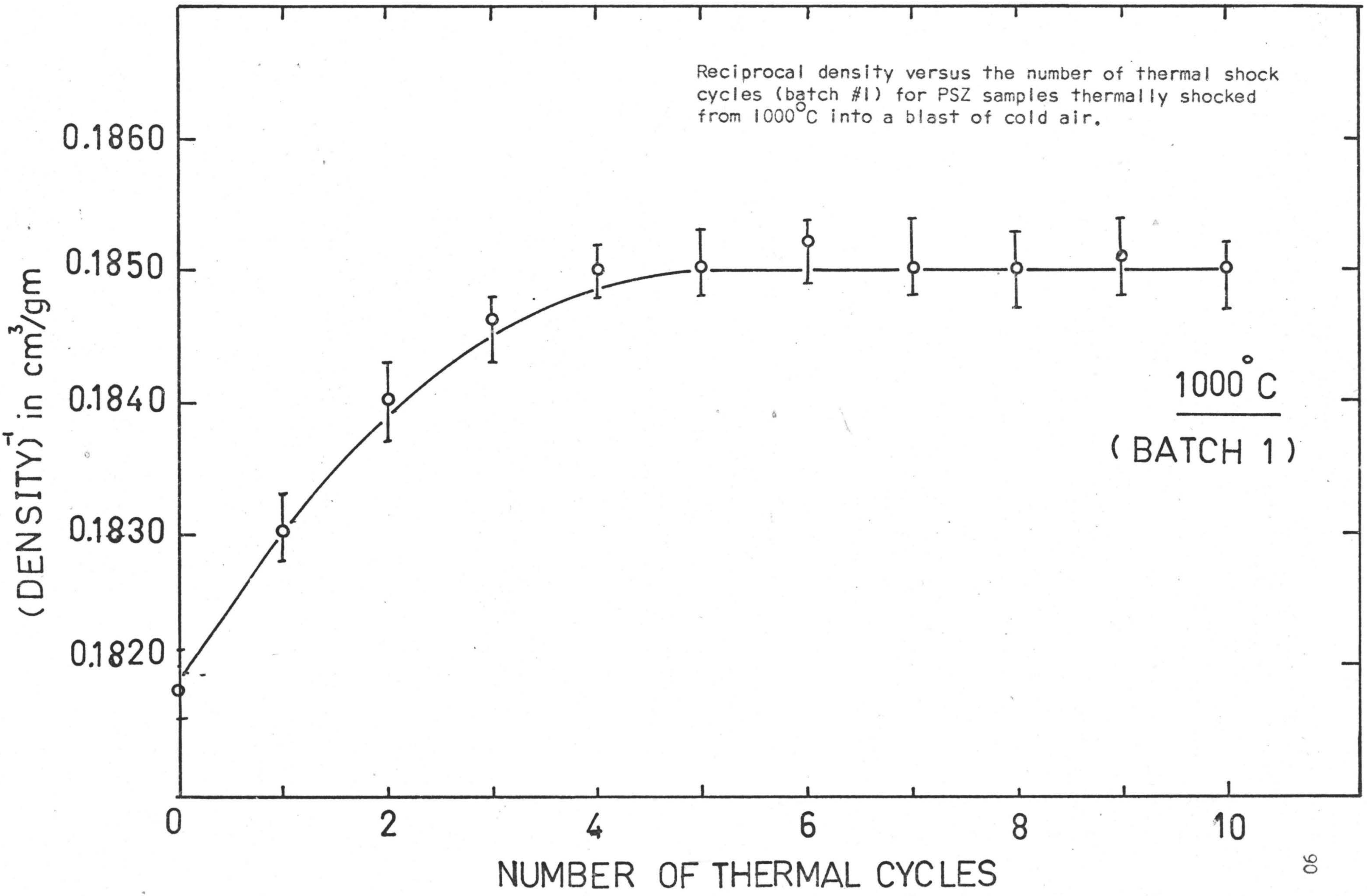

Reciprocal density versus the number of thermal shock cycles (batch #1) for PSZ samples thermally shocked from 1000°C into a blast of cold air.

FIG. 41

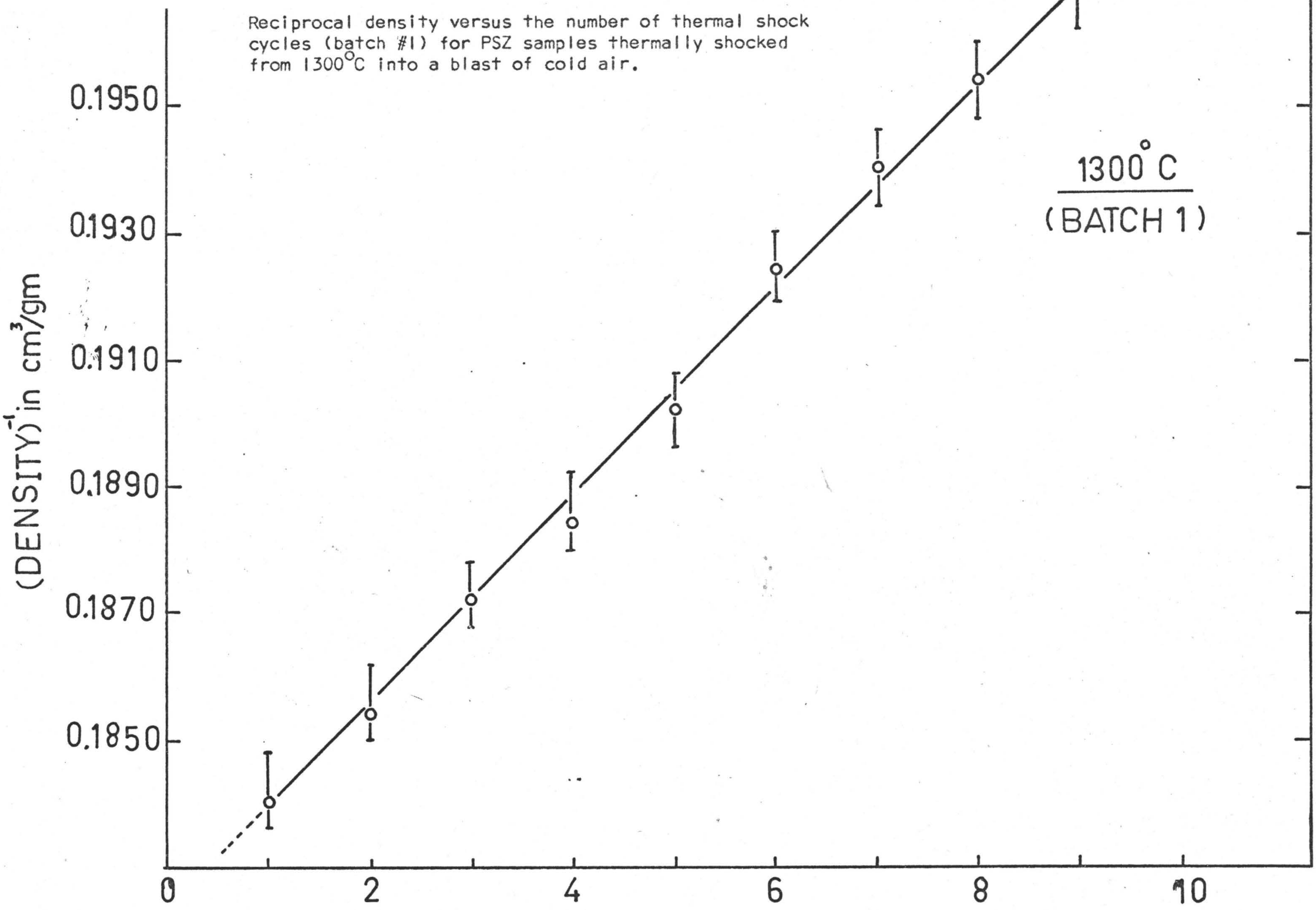

Reciprocal density versus the number of thermal shock cycles (batch #1) for PSZ samples thermally shocked from 1300°C into a blast of cold air.

FIG. 42

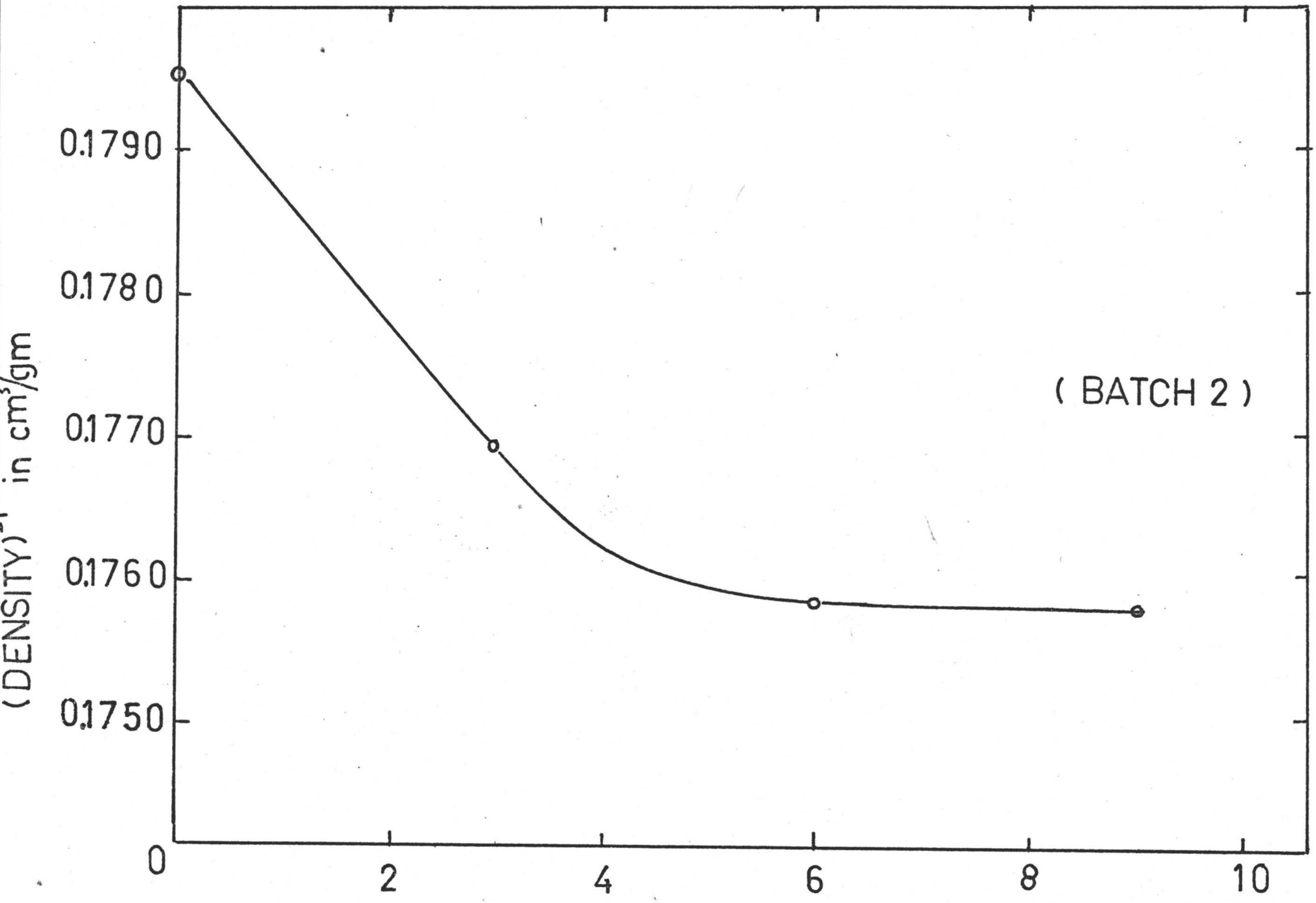

FIG.43

1/Density vs. Number of Thermal Shock Cycles for PSZ Samples Shocked from 900°C into Cold Water.

temperatures provided the temperature of the billet is fluctuated sufficiently to induce the phase transformation. An analogous mechanism is being suggested here for the increase of density of batch #2 on thermal cycling.

Twins were observed to form in this material at all temperatures used for thermal shock, and it has been suggested that the appearance of these twins at temperatures below those normally associated with the t → m transformation is evidence for the stress-induction of the transformation in this material. The process of twinning the monoclinic material and the plastic flow of the cubic matrix as evidenced by the density increase, could lower the level of internal stress in the material. This lowering could again result in cessation of the stress induction of the transformation following a given number of shock cycles. If this were the case, the number of twins on the replicas should increase to a constant value and then maintain this value for subsequent thermal shock cycles. A linear-intercept technique was used to determine the density of twins on the replicas as a function of the number of thermal shock cycles for samples at temperatures above and below the normal transformation temperature range. The data gathered are shown in Figures 44 - 46. It is evident that at 700°C and 1000°C the density of twins on the replicas reached a constant value after the first few thermal shock cycles. At temperatures above the normal transformation temperature the transformation will occur with every thermal shock as it is thermodynamically induced and therefore one can expect the density of twins to progressively increase with increasing number of thermal cycles. The data for the 1300°C shock samples agree with this observation as can be seen in Figure 31.

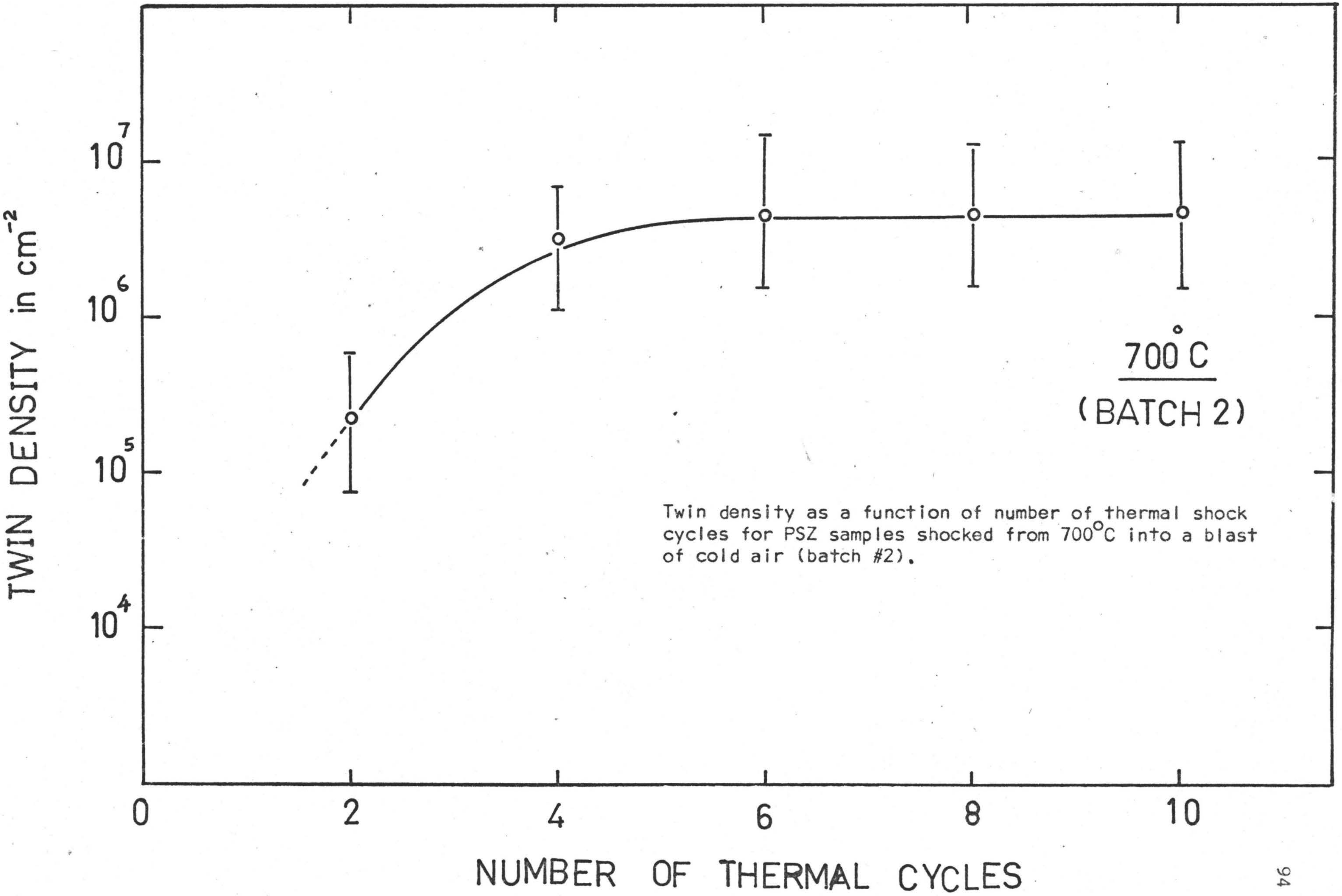

Twin density as a function of number of thermal shock cycles for PSZ samples shocked from 700°C into a blast of cold air (batch #2).

FIG. 44

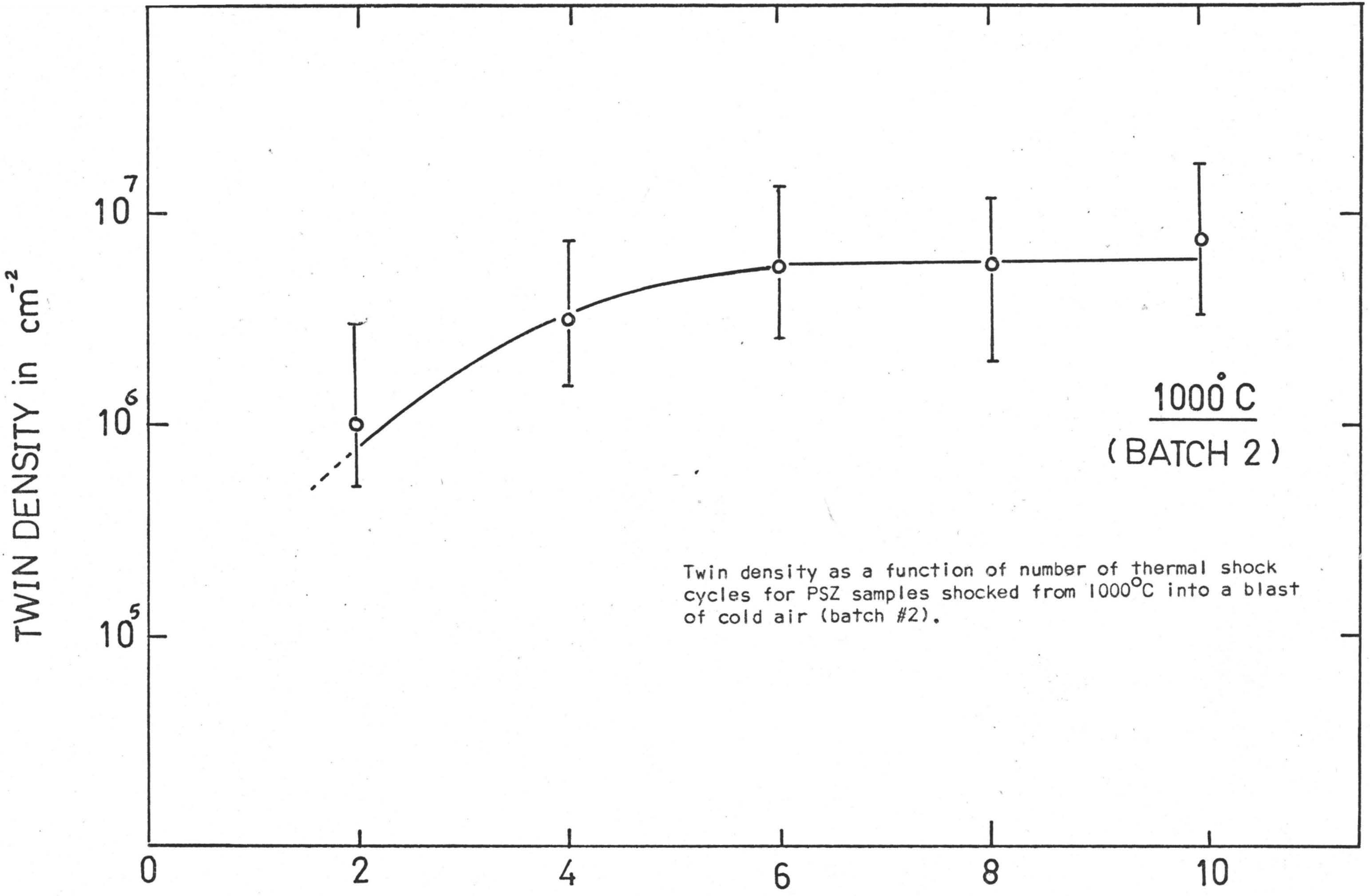

Twin density as a function of number of thermal shock cycles for PSZ samples shocked from 1000°C into a blast of cold air (batch #2).

FIG.45

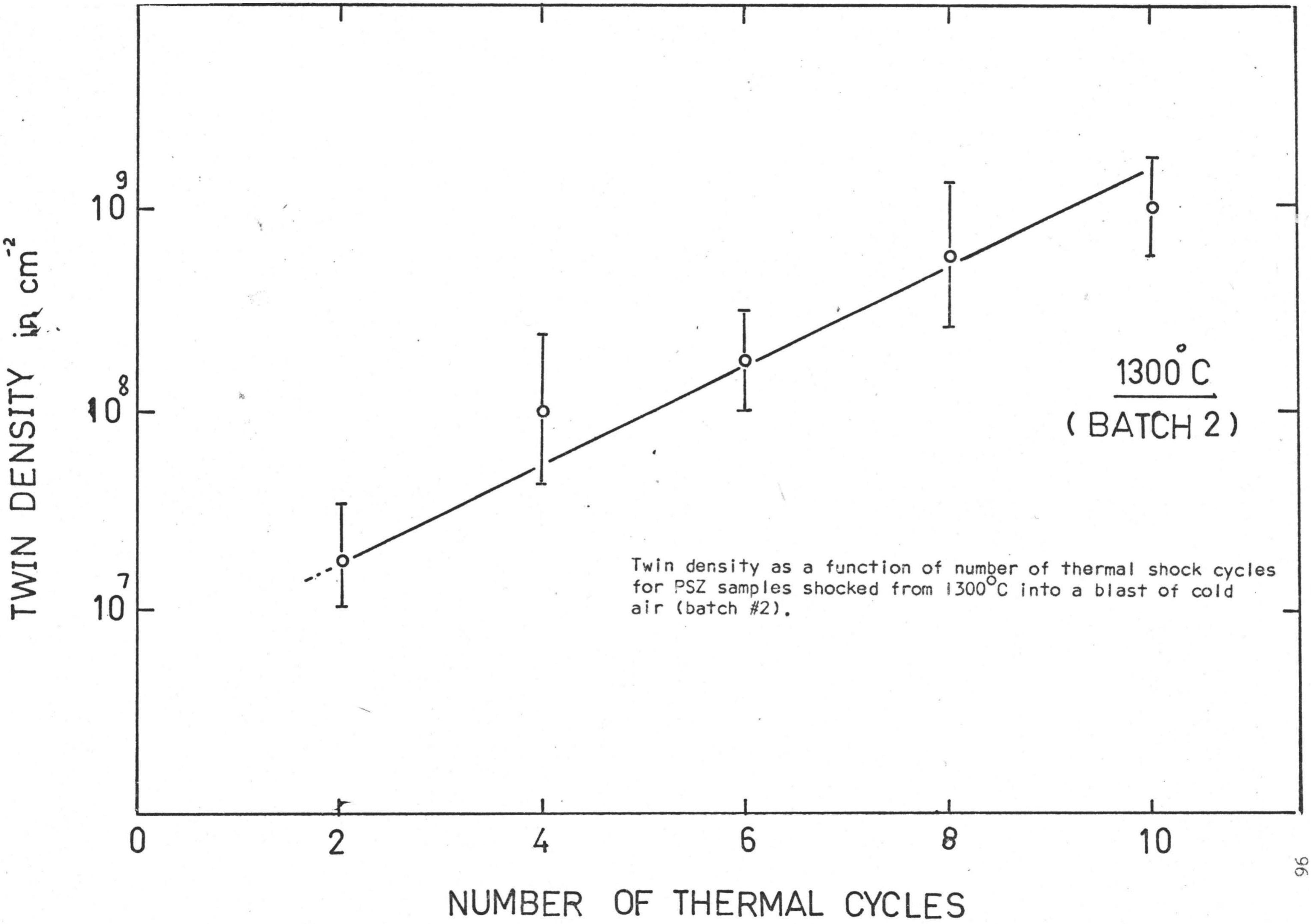

Twin density as a function of number of thermal shock cycles for PSZ samples shocked from 1300°C into a blast of cold air (batch #2).

FIG. 46

CHAPTER V

SUMMARY AND CONCLUSIONS

The objective of this work was to investigate the stress relieving mechanisms in two different batches of thermal-shock resistance CaO-PSZ. It was found that the materials have a complex subgrain structure. These subgrains are probably composed of a mixture of cubic and monoclinic domains. The nature of the stress relief in the two materials appears to result from the transformation of the pure ZrO_2 component of the microstructure at temperatures below, within and above the normal transformation temperature region.

Batch #I

(i) Production of extensive microcracking on the surface has been observed for larger ΔT-shocked samples of this batch. This material contains a larger volume fraction of monoclinic ZrO_2 than the second batch. Therefore the cubic matrix material contains more CaO and is "harder". It therefore behaves in a "brittle" fashion resulting in the production of the observed microcracks on shocking. The mechanism of production of these microcracks has been discussed based on a previously developed model. It is suggested that due to their large numbers, the cracks only propagate quasistatically and the body maintains a large portion of its strength even after continuous thermal cycling.

Batch #2

The batch #2 material contains considerably less monoclinic ZrO_2 than batch #1, and the evidence suggests that the cubic matrix behaves in a ductile fashion in this material.

(i) It was found that bumps were formed on the surfaces of the samples thermally shocked from all temperatures. It is suggested that this "blistering" phenomenon is possibly due to sub-surface deformation which could throw-up the surface in this fashion.

(ii) Large platelets with an internal bump structure were observed on replicas taken from samples thermally shocked from 1300°C into a blast of cold air for 3 cycles. It was found that during subsequent cycles these platelets coalesce. It would appear that the production of these features is associated with a macroscopic shear transformation resulting from the levels of internal stress in the material combined with the applied thermal shock. It is possible that the first few cycles "texture" the pure ZrO_2 in such a way as to allow gross platelet development on further application of the stress.

(iii) Structural twinning was observed to occur at both sub- and super-transition temperatures. The nature of the twin production was investigated and it appears that stress plays a major role in the development of these twins, suggesting that they are deformation twins. As twinning is known to accompany the transformation of t $\rightleftarrows$ m ZrO_2, the observation of such twins at sub-transformation temperatures suggests that the transformation has occurred at such temperatures. This is considered as evidence in support of the stress induced transformation concept.

(iv) Density measurements were made on thermally shocked samples of batch #1, and it was found that the reciprocal density data obtained correlated well with ratchetting phenomena studied on the same material. However, batch #2 material showed an increase in density to a constant value on thermal shock from 900°C. It is suggested that the high level of cubic phase in this material and its possible ductility could lead to an internal hot-pressing process in which the compression is supplied by the t → m transformation, and this could lead to filling up of residual fabrication porosity which led to increasing the density in this material.

REFERENCES

1. Kingery, K. D., J. Am. Ceram. Soc., 38, 3 (1955).
2. Cooke, R. G., and Lloyd, D. E., "Fabrication of Zirconia Bodies and Some Considerations of their Thermal Shock Properties", Spec. Ceramics 5, Brit. Ceram. Res. Ass., London (1972).
3. Karaulov, A., Grebenzuk, A., and Rudyak, I., Izv. Akad. Neuk SSSR, Neorg. Mat., 3, 1101 (1967).
4. Garvie, R. C., and Nicholson, P. S., J. Am. Ceram. Soc., 55, 278 (1972).
5. King, A., and Yavorski, P., J. Am. Ceram. Soc., 51, 38 (1968).
6. Garvie, R. C., Fall Meeting, Basic Science Div., Am. Ceram. Soc., Ottawa (1969).
7. Hart, J. L. and Chaklader, A. C., Mater. Res. Bull., 2 521 (1967).
8. Viechnicki, E., and Stubican, V., J. Am. Ceram. Soc., 48, 292 (1965).
9. Wells, A. F., "Structural Inorganic Chemistry", Oxford, London (1962).
10. Bendoraitis, J. G., and Salmon, R. E., J. Phys. Chem., 69, 3666 (1965).
11. Yardley, K., Miner. Mag., 21, 169 (1926).
12. Naray-Szabo, St., Z. Krystallogr., 94, 414 (1936).
13. McCullough, J. D., and Trueblood, K. N., Acta Cryst., 12, 507 (1959).
14. Smith, D. K., and Newkirk, H. W., Acta Cryst., 18, 983 (1965).
15. Smith, C. F., and Crandall, W. B., J. Am. Ceram. Soc., 47, 624 (1964).
16. Campbell, W. J., and Grain, C. F., U. S. Bur. Mines RI5982, (1962).
17. Lang, S. M., Franklin, E. W., and Tylutki, N. J., Aerospace Research Laboratories Rept. No. ARL-65-40 (1965).

18. Ruff, O., and Ebert, F., Zlschr. Anorg. Allgem. Chem., 180, 19 (1929).

19. Teufer, G., Acta Cryst., 15, 1187 (1962).

20. J. Krstanovic, J. Am. Ceram. Soc., 38, 12 (1955).

21. Lang, S. M., J. Am. Ceram. Soc., 47, 641 (1964).

22. Smith, D. K., and Cline, C. F., J. Am. Ceram. Soc., 45, 249 (1962).

23. Wolten, G. M., J. Am. Ceram. Soc., 46, 418 (1963).

24. Duwez, P., Odell, F., and Brown, F. J., J. Am. Ceram. Soc., 35, 107 (1952).

25. Dietzel, A., and Tober, H., Ber. Deut. Keram. Ges., 30, 47 (1953).

26. Cocco, A., and Schromek, N., Radex Rundschau, No. 3, 590 (1961).

27. Grain, C. F., J. Am. Ceram. Soc., 50, 288 (1967).

28. Roy, R., Miyabe, H., and Diness, A., "Subsolidus Decompositon of CaO-Stabilized ZrO_2", 66th Annual Meeting, Am. Ceram. Soc., (1964).

29. Fernandes, S., and Beaudin, L., "Subsolidus Equilibria in the CaO-ZrO_2 System", Annual Pittsburgh Diffraction Conference, (1963).

30. Barbariol, I., Ann. D. Chim., 55, 321 (1965).

31. Garvie, R. C., J. Am. Ceram. Soc., 51, 553 (1968).

32. Delamarre, C., and Yorba, M., Rev. Hautes Temper. et Refract., 2, 313 (1965).

33. Garvie, R., "High Temperature Oxides", 2, New York, 117 (1970).

34. Sukharevskii, B., Vishnevskii, I., and Gavrish, A., Dokl. Akad. Nauk. SSSR, 140, 884 (1961).

35. Weber, B. C., Garrett, H. J., Mauer, F. A., and Schwartz, M. A., J. Am. Ceram. Soc., 39, 197 (1956).

36. Buckley, J. D., and Wilson, H. H., J. Am. Ceram. Soc., 46, 510 (1963).

37. Kauer, E., Klinger, O., and Rabenan, A., Ztschr. Electrochem., 63, 927 (1959).

38. Murray, P., and Allison, E., Trans. Brit. Ceram. Soc., 53, 335 (1954).

39. Wolten, G. M., Acta Cryst., 17, 763 (1964).

40. Cohen, I. and Schaner, B. E., J. Nucl. Mater. 9, 18 (1963).

41. Evans, P. E., and Wildsmith, G., Nature, 189, 569 (1961).

42. Fehrenbacher, L. L., and Jacobson, L. A., J. Am. Ceram. Soc., 48, 157 (1965).

43. Kaufman, L., and Cohen, M., "Thermodynamics and Kinetics of Martensitic Transformation", Prog. Met. Phy., 7, 165 (1958).

44. Kaufman, L., and Cohen, M., Trans. AIME, 206, 1393 (1956).

45. Lieberman, D. S., The Mechanism of Transformation in Metals, Institute of Metals Monograph and Report Series No. 18 (1955).

46. Bunshah, R. F., and Mehl, R. F., Trans. AIME, 197, 1251 (1953).

47. Edmondson, B., and Ko, T., Acta Met., 2 235 (1954).

48. Kulin, S. A., and Speich, G. R., Trans. AIME, 194, 258 (1952).

49. Holden, A. N., Acta Met., 1, 617 (1952).

50. Shih, C. H., Averbach, B. L., and Cohen, M., Trans. AIME, 203, 183 (1955).

51. Scheil, E., Z. Anorg. Chem., 207, 21 (1932).

52. McReynolds, A. W., J. Appl. Phys., 20, 896 (1949).

53. Kulin, S. A., Cohen, M., and Averbach, B. L., Trans. AIME, 194, 661 (1952).

54. Patel, J. R., and Cohen, M., Acta Met., 1, 531 (1953).

55. Bailey, J. E., Proc. Roy. Soc., A279, 395 (1964).

56. Buerger, M. J., "Phase Transformations in Solids", Wiley, New York (1951).

57. Kelly, P. M., and Nutting, J., Proc. Roy. Soc. A259, 45 (1960).

58. Hull, D., Phil. Mag., 7, 537 (1962).

59. Swan, P. R., and Warlimont, H., Acta. Met., 11, 511 (1963).

60. Grain, C. F., and Garvie, R. C., U.S. Bur. Mines, RI6619, (1965).

61. Ubbelohde, A. R., Quart. Rev., Chem. Soc., 11, 246 (1956).

62. Bansal, G. and Heuer, A., "Martensitic Phase Transformation in Zirconia", 74th Annual Meeting, Am. Ceram. Soc., Washington D.C. (1972).

63. Dow Whitney, E., J. Am. Ceram. Soc., 45, 612 (1962).

64. Dow Whitney, E., J. Electrochem. Soc., 112, 91 (1965).

65. Vahldiek, F. W., Robinson, L. B., and Lynch, C. T., Science, 142, 1059 (1963).

66. Kulcinski, G. L., and Maynard, W. C., J. Appl. Phys., 37, 3519 (1966).

67. Kulcinski, G. L., J. Am. Ceram. Soc., 51, 582 (1968).

68. Garvie, R. C., J. Phys. Chem., 69, 1238 (1965).

69. Maiti, H. S., Gokhale, K. V., and Subbarao, E. C., J. Am. Ceram. Soc., 55, 317 (1972).

70. Green, D. J., "Fracture Toughness of CaO-PSZ", M.Sc. Thesis, McMaster University (1972).

71. Duhamel, J. M., Memoirs de l' Institute de France, 440, (1838).

72. Boley, B. A., and Weiner, J. H., "Theory of Thermal Stresses", John Wiley and Sons, Inc., New York, (1960).

73. Kingery, W. D., J. Am. Ceram. Soc., 38, 3 (1955).

74. Hasselman, D. P., J. Am. Ceram. Soc., 46, 229 (1963).

75. Hasselman, D. P., J. Am. Ceram. Soc., 49, 103 (1966).

76. Hasselman, D. P., J. Am. Ceram. Soc., 50, 454 (1967).

77. Hasselman, D. P., J. Am. Ceram. Soc., 46, 535 (1963).

78. Nakayama, J., and Ishizuka, M., Bull. Am. Ceram. Soc., 45, 666 (1966).

79. Hasselman, D. P., J. Am. Ceram. Soc., 52, 600 (1969).

80. Berry, J. P., J. Mech. Phys. Solids, 8, 206 (1960).

81. Curtis, C. E., J. Am. Ceram. Soc., 30, 180 (1947).

82. Jaeger, R., and Nickel, R., "Ceramics in Severe Environments", Raleigh, N. C., (1970).

83. Bansal, G., and Heuer, A., "Deformation Sub-Structure in Unstablized Zirconia", 72nd Annual meeting, Am. Ceram. Soc., Philadelphia (1970).

84. Williams, R. C., and Wyckoff, R. W., Science, 101, 594 (1945).

85. A. Kontopoulos and P. S. Nicholson, J. Am. Ceram. Soc., 54, 317 (1971).

86. A. C. D. Chaklader, Am. Ceram. Soc. Bull., 44, 1965.